# A DYNAMIC PERFORMANCE ANALYSIS OF A HYDRAULICALLY OPERATED ANGULAR CONTROL SYSTEM

A THESIS

Presented to

The Faculty of the Division of Graduate

Studies and Research

By

Stanley Wayne Zieg

In Partial Fulfillment

of the Requirements for the Degree

Master of Science in Mechanical Engineering

Georgia Institute of Technology

December, 1973

A DYNAMIC PERFORMANCE ANALYSIS OF A HYDRAULICALLY

OPERATED ANGULAR CONTROL SYSTEM

Approved:

Dr. S. L. Dickerson, Chairman

Dr. Tom White

Dr. W. D. McLeod

Alan L. Wilcox

Mr. Alan L. Wilcox

Date approved by Chairman: 9-11-73

## ACKNOWLEDGMENTS

The author would like to express sincere thanks to Dr. Stephen L. Dickerson for his willing suggestions and continual availability in helping to resolve the many problems encountered in the completion of a thesis. Thanks are also extended to Dr. W. D. McLeod and Dr. Tom White for their services as members of the thesis reading committee.

Special thanks are given to Scientific-Atlanta, Inc., for the use of their facilities and equipment in the research for this thesis. In particular, thanks are due to Mr. Alan Wilcox who has contributed much time and information regarding the specifics of the problem area.

Finally, the author wishes to thank his wife, Diane, whose love, encouragement, and confidence have been a continual incentive throughout his graduate work.

TABLE OF CONTENTS

# LIST OF ILLUSTRATIONS

LIST OF ILLUSTRATIONS (Continued)

# NOMENCLATURE

| | |
|---|---|
| $A$ | Area of piston |
| $A_o$ | Area of orifice |
| $A_s$ | Area of spool |
| $C_L$ | Capacitance of hydraulic line |
| $f_k$ | Kinetic moment of turntable |
| $f_s$ | Static moment of turntable |
| $I$ | Inertia of turntable and load |
| $i_i$ | Ideal current of controller |
| $I_L$ | Inertia of hydraulic line |
| $k_c$ | Variable gain of controller |
| $k_i$ | Constant (i = 1, 7) |
| $k_B$ | Bearing viscous friction coefficient |
| $k_f$ | Net stiffness of armature - flapper |
| $k_v$ | Valve gain coefficient |
| $k_w$ | Feedback wire stiffness |
| $L$ | Leakage coefficient of cylinder |
| $L_c$ | Inductance of coil |
| Lch | Length of chain |
| Lcy | Length of cylinder |
| $M_{ext}$ | External moment applied to turntable |
| $p$ | Pressure |
| $p_1$ | Pressure of cylinder A |
| $p_2$ | Pressure of cylinder B |

| | |
|---|---|
| $p_r$ | Reservoir pressure |
| $p_s$ | Supply pressure |
| $q_1$ | Flow rate to cylinder A |
| $q_2$ | Flow rate to cylinder B |
| $q_c$ | Flow due to compression of fluid |
| $q_d$ | Flow due to displacement of piston |
| $q_i$ | Flow into piston |
| $q_\ell$ | Flow due to leakage of cylinder |
| $q_r$ | Return flow from valve |
| $q_s$ | Supply flow to valve |
| R | Pitch radius of sprocket |
| $R_c$ | Resistance of coil |
| $R_L$ | Resistance of hydraulic line |
| $v_L$ | Hydraulic fluid velocity |
| $v_s$ | Velocity of spool |
| x | Displacement of piston |
| $x_s$ | Displacement of spool |
| $\beta$ | Bulk modulus of fluid |
| $\Delta p$ | Differential pressure across orifice |
| $\varepsilon$ | Error signal between actual and desired displacement |
| $\gamma$ | Specific weight of fluid |
| $\rho$ | Fluid density |
| $\tau_c$ | Time constant of controller |
| $\theta$ | Angular displacement |
| $\omega$ | Angular velocity |
| $\omega_{hp}$ | Natural frequency of second stage of valve |

$\omega_n$ Natural frequency of first stage of valve

$\zeta_{hp}$ Damping ratio of second stage of valve

$\zeta$ Damping ratio of first stage of valve

## SUMMARY

This study deals with a mathematical analysis of a hydraulic positioning system. The purpose of this analysis was to determine the ultimate operational limits for a particular hydraulic system and to investigate methods of increasing this performance.

In the mathematical modelling, two models were used to describe the system performance. A non-linear model was developed which incorporated all nonlinear effects seen as significant by the author. A linear model, based on the non-linear model, was developed to examine the possible accuracy of the much simpler linear model and the effects of the various non-limiting.

The non-linear model was shown to have dynamic operating characteristics in very close agreement with actual test data. The major effect limiting system response was shown to be valve flow saturation. Of lesser, but nevertheless significant, effect, stiction of the bearing and the square-root law governing flow through the valve caused the linear and non-linear models to vary in their dynamic response. For an extremely small error signal, the linear and non-linear models were in agreement.

The linear model was used to examine the effect of altering several system parameters. This parameter variation showed that, while the exact determination of leakage and viscous bearing friction coefficients is not critical in the prediction of system performance, the values of system gain and load inertia have a significant impact on the dynamic characteristics of the system.

# CHAPTER I

## INTRODUCTION

In recent years, hydraulic systems have often been utilized to fill the need for powerful, quickly acting actuation systems. As the performance of these hydraulic systems increases, the cost of constructing such a system has increased. Thus the desirability of being able to predetermine the dynamic operating characteristics of a proposed hydraulic system is obvious. The purpose of this thesis is to establish the performance limitations of a particular hydraulic system and to indicate the reasons for these limitations.

The major problem in any theoretical analysis of a hydraulic system is analyzing the many non-linearities inherent in such a system. Also, as the degree of accuracy required increases, the number of non-linearities which are significant increases. Classical control theory is normally sufficient to predict the system performance as long as multiple non-linearities do not occur. When these non-linearities appear, the classical techniques become so unwieldly that a valid analysis is virtually impossible. Modern control theory, however, is able to deal with these problems with relative ease. The state variable approach permits simulation of such a dynamic system directly on a digital computer without it being necessary to ever explicitly solve the expressions relating the dynamics of the system. Although this technique can give very accurate information for a properly modeled system, it cannot substitute for good engineering to establish a correct model.

Due to the fact that the analysis of a complete hydraulic system using classical techniques is not easily accomplished for any but the most simple systems and because modern control theory is a relatively recent development, most work in the field of hydraulics has been directed toward developing accurate models of the individual system components rather than in analyzing complete systems. One of the most thorough dealings with the entire field of fluid power is a series of papers published by members of the Dynamic Analysis and Control Laboratory at Massachusetts Institute of Technology. Many of these papers, including the "Contribution to Hydraulic Control" series, have been published in the book Fluid Power Control (1). Although hundreds of similar efforts have been directed at predicting the dynamic operating characteristics of individual components, little has been done in the area of combining these improved, mostly non-linear, models into a system analysis. One relatively complete closed loop system analysis was carried out by Rausch in 1959 (2). In his study, non-linear models were developed and a non-linear analog solution was compared with a linearized classical control solution to the same problem, with disappointing results.

Often, advances in hydraulics have been brought about by advances in other fields. This has especially been the case in the aerospace industry. Electronic radar and communication equipment have advanced to such a sophistication that analyzing the performance of this equipment using a scale model of the airplane or spacecraft has been a necessity for several years. Recently, angular displacements of one-tenth of a milliradian have become possible to detect with this electronic equipment. The test equipment must therefore have the capability to detect and

respond to such a small displacement. In the past, turntables to which the scale models are mounted have been driven by electric motors. When high torques are also required, these electric motors and their associated geartrains are able to respond neither fast nor accurately enough for these small displacements. Hydraulics has recently been considered as a means of meeting this requirement.

Electronic testing equipment such as needed in the aerospace industry is one of the major product areas of Scientific-Atlanta, Inc., an Atlanta based electronics firm. Responding to the need for a high torque antenna positioner for extremely accurate or smooth operation, a hydraulic system was designed and two units were built by this firm. One of these positioners is shown in Figure 1.

The problem to which this thesis is directed is that of mathematically describing the particular system as constructed by Scientific-Atlanta and simulating the system on a digital computer. The simulation will include both a non-linear description and a linearized description about various operating points. Each will be compared with data from tests of the actual system. The purpose of this thesis is to illustrate the ultimate limitations on the performance of the hardware and what effects cause these limitations. With this information, modifications can be made to the existing or subsequent positioning systems to increase the performance beyond that of the two prototypes.

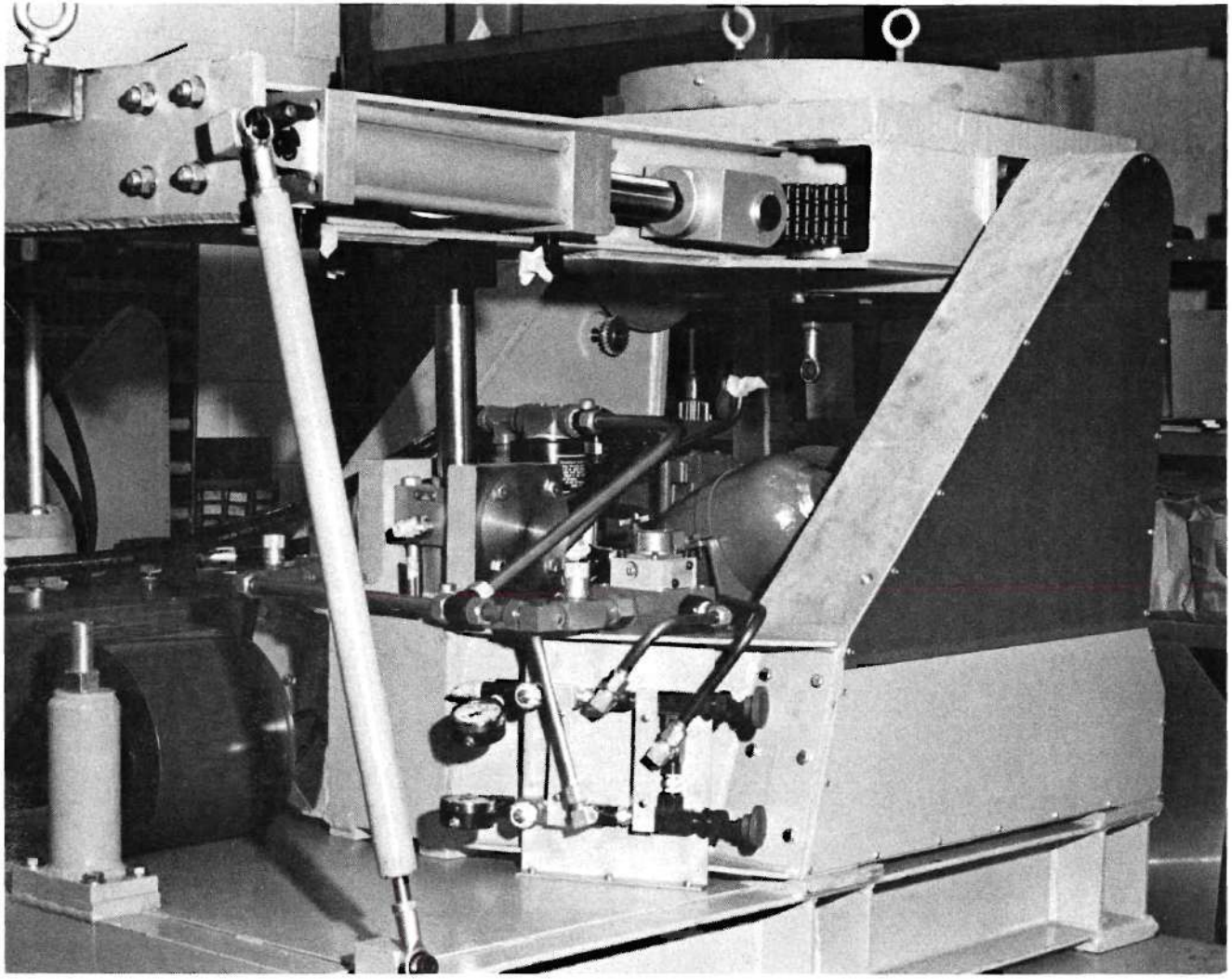

Figure 1. Hydraulic Antenna Positioner.

# CHAPTER II

## THEORETICAL ANALYSIS

The approach used in the analysis of the hydraulic servo system is as follows. Each component of the servo system is modeled separately, including all dynamic effects which seem to be significant. Once all of the individual components are modeled, they are combined to form the entire system. The system consisting of all the interacting components is then analyzed to determine which of the dynamic effects can be neglected at lower operating frequencies.

A schematic diagram of the entire configuration may be seen in Figure 2. A commercial servo-controller is used to compare the desired angular position with the feedback signal from the turntable assembly. The output of this amplifier is fed to a four-way, two-stage electro-hydraulic valve which controls the flow of fluid leading to a pair of hydraulic cylinders. These cylinders drive the turntable by a chain and sprocket drive mechanism. In the intended application, a scale model aircraft would be mounted to the turntable and rotated through various angles. The angular displacement is detected by a ten turn potentiometer coupled to the turntable by a geartrain. A slight valve underlap will enable both pistons to be pressurized when the system is in operation. Because a highly accurate geartrain is utilized, mechanical backlash is minimized.

In the following paragraphs, the mathematical model for each component is presented. All dynamic and non-linear effects considered

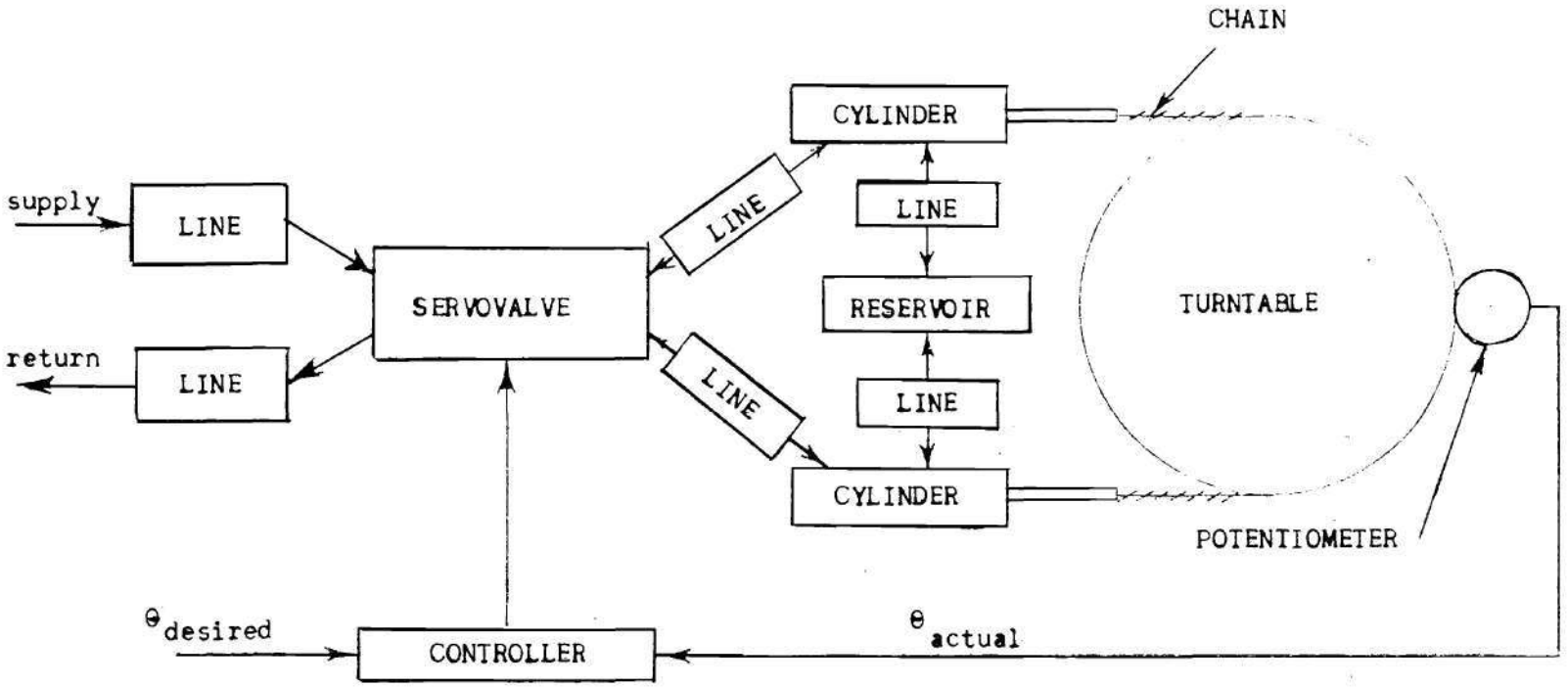


Figure 2. Block Diagram of a Hydraulic Positioning System.

significant by the author are discussed and included in the analysis. However, later some of these effects may be shown to be minimal.

## Servo-Controller

The commercial controller used in this system can be represented by a simple lag model as long as saturation of the output does not occur. The output may be saturated in either current or voltage.

To develop the linear and non-linear models of this element of the system, the idealized output current is found first. This represents the linear model since no saturation is allowed. The idealized model may be represented by the transfer function

$$\frac{i_i(s)}{\varepsilon(s)} = \frac{k_c}{\tau_c s + 1} \qquad (2.1)$$

where

$i_i$ = output current, ma.

$k_c$ = variable gain of controller, 2.5 to 250 ma/volt.

$\tau_c$ = time constant of controller.

$\varepsilon$ = error signal between desired and actual angular displacement, volts.

If non-linear saturation of the controller is to be considered, the block diagram of Figure 3 represents the entire saturated controller. The implementation of these and other non-linearities in the simulation model are discussed in Appendix B.

## Servovalve

Analytic representation of servovalve performance has been the subject of much study and research in recent years. Although high order

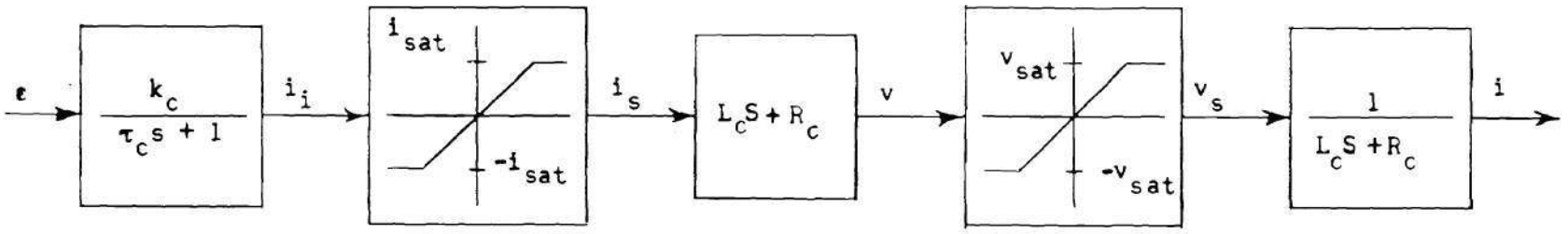


where: $i_{sat}$ = saturation current, ma.

$L_c$ = load inductance, henrys.

$R_c$ = load resistance, ohms.

$v_{sat}$ = saturation voltage, mv.

Figure 3. Block Diagram of Servo-Controller.

models have been developed to account for the many dynamic effects in a two stage valve, the many significant non-linearities of the valves together with the extremely high frequency of some of these effects tends to make lower order models more satisfactory. To derive the appropriate transfer function for this application, two models of this type of valve, presented by Merritt (3) and Moog (4), were combined into a more complete model which includes the dynamics of the flapper and the spool. Also current is considered an input. The development of this model is in Appendix A.

A frequency response analysis of the composite model described above, as well as the third order Moog model of Figure 33, Appendix A, are compared in Figure 4 with the second order model suggested by Moog (5).

The discrepancy among the three curves at higher frequencies is apparently due to a discrepancy in the data supplied by the valve manufacturer. Since the second order model is based upon experimental evidence, this model was used in the analysis.

Two effects are not considered in the linear transfer function which must be considered in the non-linear analysis. The first involves the physical limitation in movement of the spool and the second involves the flow rates to the two cylinders. Each will be discussed separately.

The transfer function derived in Appendix A for the servovalve expressed in block diagram form in Figure 5. For a description of state variable format, see Appendix C. Valve flow forces were not considered in this analysis. If $x_s$ reaches a mechanical limit, two non-linear effects must be implemented. $X_s$ has reached a maximum and regardless of the input

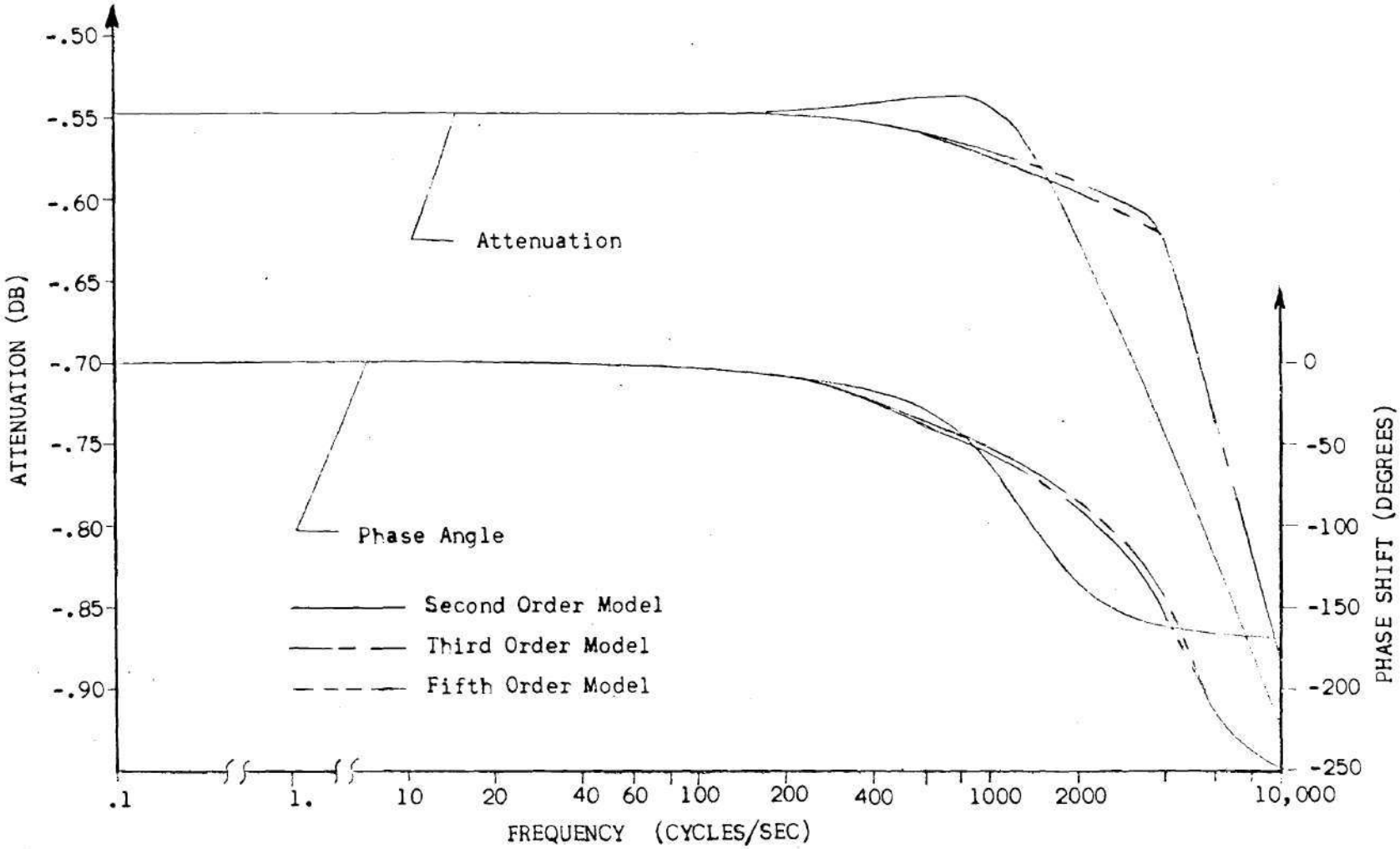


Figure 4. Bode Plot for Second, Third, and Fifth Order Moog Valve Models.

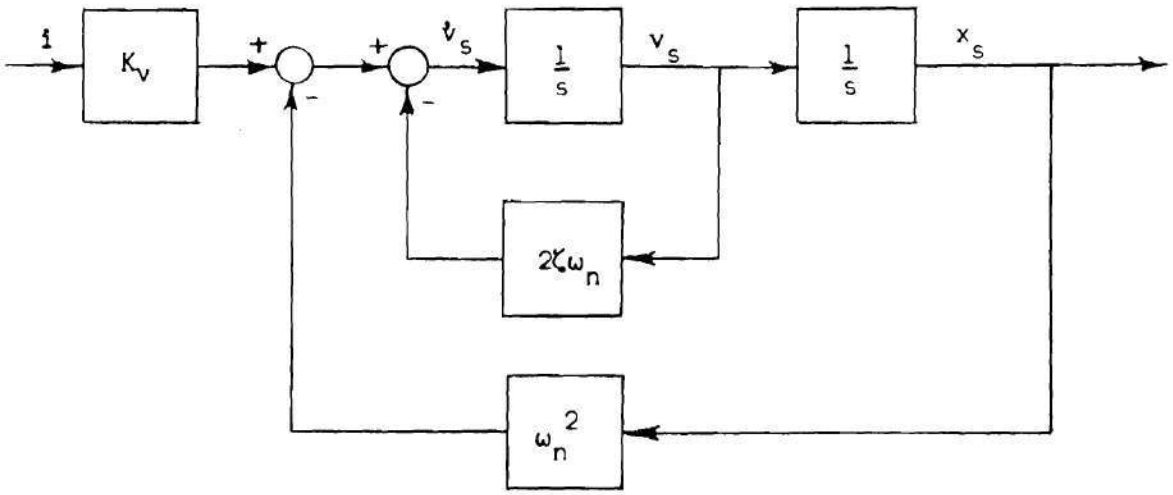


Figure 5. Linear Block Diagram of Servovalve

to the integrator its velocity is zero. The velocity again becomes non-zero only when $\dot{v}_s$ acquires the proper sign to bring $X_s$ within the unsaturated limits. A non-linear representation of this may be seen in Figure 6.

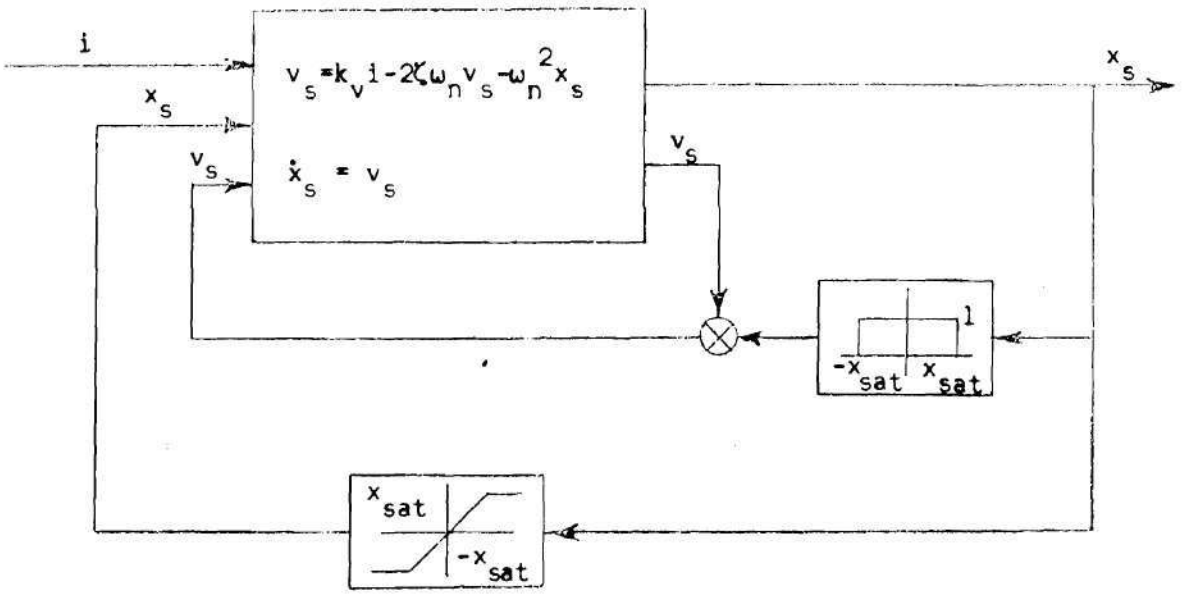


Figure 6. Non-linear Block Diagram of Servovalve

where $X_{sat}$ = saturation spool displacement. The net results of the above diagram are that velocity remains unchanged as long as spool displacement is not at a maximum and that spool displacement is saturated if it reaches the maximum.

Commonly, flow to and from the valve are assumed to be equal. Because line transients are to be considered in this analysis and because the flows are from two different cylinders, flows to and from the valve may not be equal at a given time. Therefore, this common assumption may not be valid in this case. A more complete pressure-flow relationship must therefore be found for the non-linear analysis.

A four-way, three-land spool valve can be presented accurately by its electrical analogy: a loaded Wheatstone bridge with square law arms (6), shown in Figure 7. The mechanical orifice configuration of Figure 8 is equivalent to the electrical network of Figure 7. Flows $q_a$, $q_b$, $q_c$, and $q_d$ are described by the orifice flow relation.

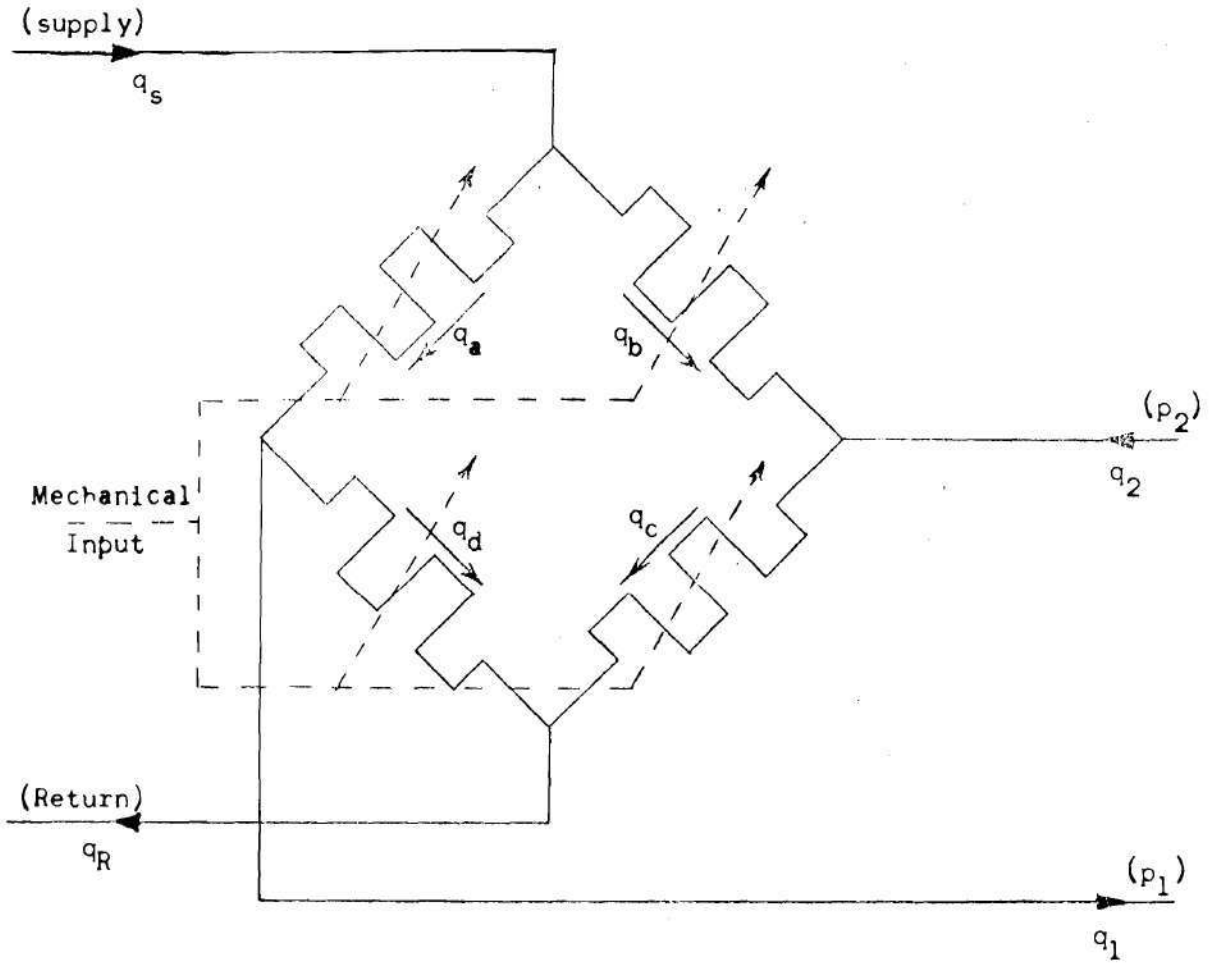


Figure 7. Electrical Analogy of Spool Valve Orifices.

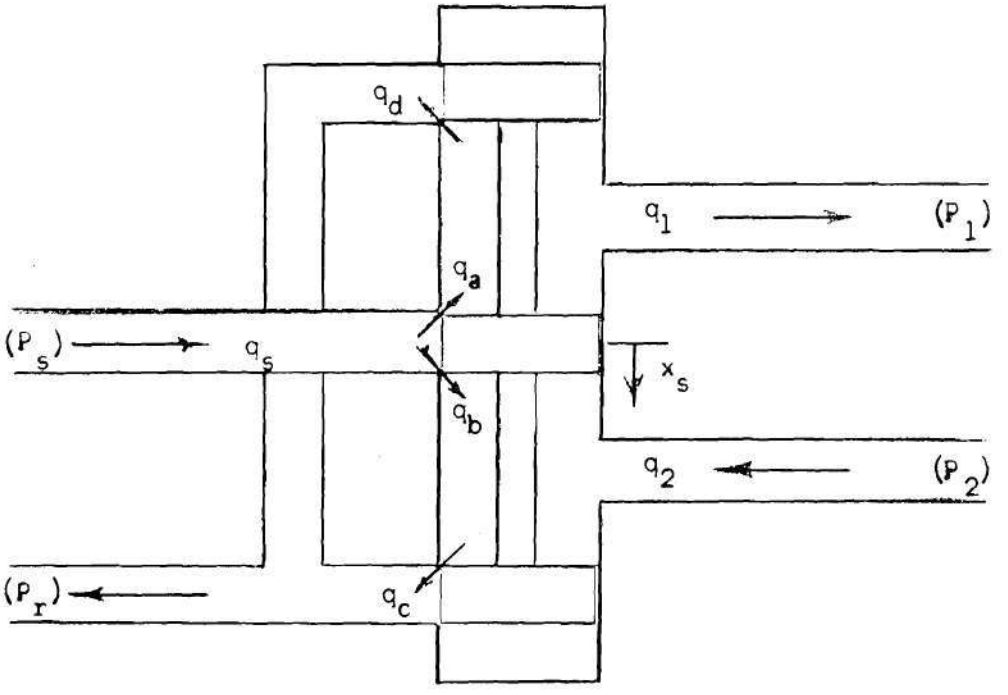


Figure 8. Four-way Spool Valve

This is

$$q = C_d A_o \sqrt{2/\rho(\Delta P)} \qquad (2.2)$$

where

$C_d$ = orifice coefficient, dimensionless.

$\rho$ = density of fluid, lb-sec$^2$/in$^4$.

$A_o$ = orifice area, in$^2$.

$\Delta P$ = differential pressure across orifice, lb/in$^2$.

$q$ = flow rate through orifice, in$^3$/sec.

Assuming the value is symmetrical with matched orifices,

$$q = k(X_s) \sqrt{P_1 - P_2}$$

where $k(X_s)$ is a linear function of spool displacement.

The flows may therefore be represented as

$$
\begin{aligned}
q_1 &= k_1(X_s)\sqrt{P_s - P_1} - k_4(X_s)\sqrt{P_1 - P_r} \\
q_2 &= -k_2(X_s)\sqrt{P_s - P_1} + k_3(X_s)\sqrt{P_2 - P_r} \\
q_5 &= k_1(X_s)\sqrt{P_s - P_1} + k_2(x_s)\sqrt{P_s - P_2} \\
q_r &= k_3(X_s)\sqrt{P_2 - P_r} + k_4(X_s)\sqrt{P_1 - P_r}
\end{aligned}
\qquad (2.3)
$$

where $k_i = C_d A_o \sqrt{2/\rho}$ is the orifice coefficient of orifice. For sharp edged square orifices, $C_d \approx .6$ (7). Assuming $\rho \approx .78 \times 10^{-4}$ lb-sec$^2$/in$^4$ for petroleum based fluids (8),

$$C_d \frac{2}{\rho} \approx 100 \quad \text{in}^2/\sqrt{16} - \text{sec}$$

$$A_o = X_s \pi d_s$$

where $d_s$ = diameter of spool, in.

Therefore

$$k(X_s) = 314\, d_s X_s$$

Assuming no leakage flow, $k(X_s) = 0$ when $A_o < 0$, $k_1$, $k_2$, $k_3$, and $k_4$ can be represented in Figure 9.

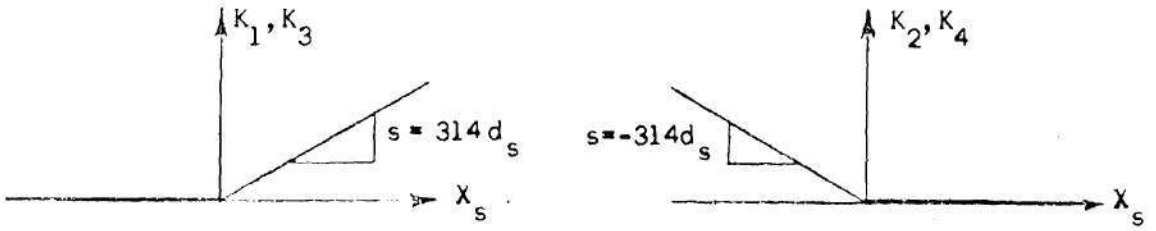


Figure 9. Flow Coefficients as Functions of Spool Displacement.

The flow equations thus simplify to

$$q_1 = 314\, d_s\, X_s \sqrt{P_s - P_1}$$

$$q_2 = 314\, d_s\, X_s \sqrt{P_2 - P_r}$$

$$q_s = 314\, d_s\, X_s \sqrt{P_s - P_1}$$

$$q_r = 314\, d_s\, X_s \sqrt{P_2 - P_r} \quad \text{for } X_s > 0 \qquad (2.4)$$

$$q_1 = 314\, d_s\, X_s \sqrt{P_1 - P_r}$$

$$q_2 = 314\, d_s\, X_s \sqrt{P_s - P_2}$$

$$q_s = 1314\, d_s\, X_s \sqrt{P_s - P_2}$$

$$q_r = 1314\, d_s X_s \sqrt{P_1 - P_r} \quad \text{for } X_s < 0$$

Using the above relations and the non-linear value dynamic equations outlined above, the non-linear description of the value is complete.

## Piston-Chain-Turntable

The pistons and turntable-chain combination must be analyzed as a unit due to the interaction of these components during motion of the system. Several assumptions have been made in the analysis of this assembly.

1. The pressure is uniform throughout each cylinder.
2. The mechanical assembly is rigid; that is, there is no relative deflection between the sprocket and turntable or between the piston mounting point and the sprocket.

3. The bearing friction is independent of angular displacement.

Continuity of flow around the cylinder yields

$$q_i = q_d + q_e + q_c \tag{2.5}$$

where $q_i$ = flow into the cylinder from the valve, $in^3/sec$.

$q_d$ = flow due to piston displacement, $in^3/sec$.

$q_e$ = leakage flow around piston, $in^3/sec$.

$q_c$ = compression of hydraulic fluid, $in^3/sec$.

Each of the above flows may be expressed by the following equations:

$$q_d = A\, dx/dt \tag{2.6}$$

A = cylinder area, $in^2$.

x = position of piston, in.

$$q_e = L(p - p_r) = Lp \tag{2.7}$$

L = leakage coefficient, $in^3/sec/lb/in^2$.

p = pressure of fluid in cylinder, $lb/in^2$.

$p_r$ = reservoir pressure = 0

$$q_c = \frac{1}{\beta} (Ax)\, dp/dt \tag{2.8}$$

where $\beta$ = bulk modulus, $lb/in^2$.

The displacement of the piston is governed by two factors: turntable displacement and stretching of the chain. Referring to Figure 10, it may be seen that if the chain is the correct length so that the pistons are centered with no pressure or angular displacement of the turntable, the displacement of piston A may be expressed as

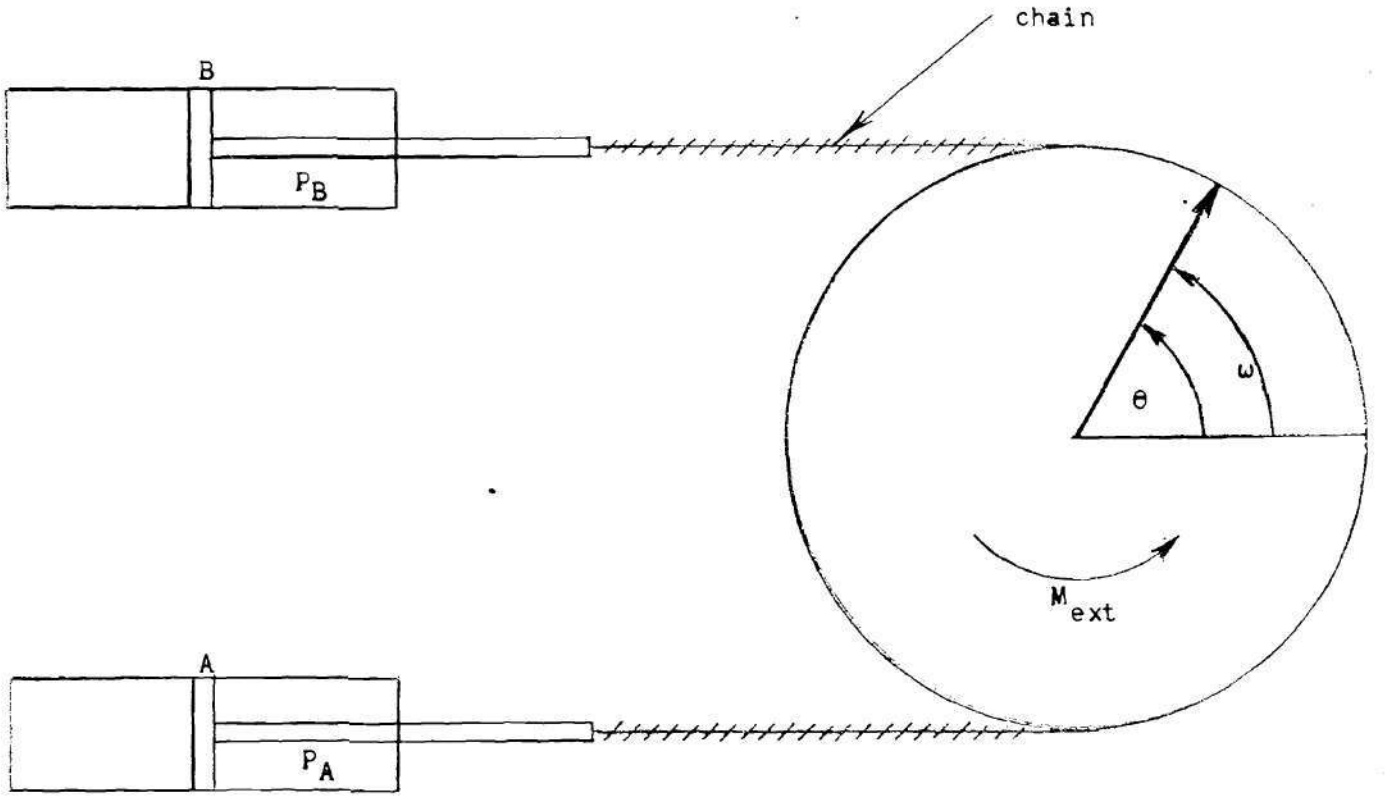


Figure 10. Mechanical Piston-Chain-Turntable Assembly.

$$X = \frac{Lcy}{2} + R\theta \tag{2.9}$$

where Lcy = Length of cylinder, in.

R = pitch radius of sprocket, in.

$\theta$ = angular displacement, radians.

The stretching of the chain adds another factor to the displacement. This stretching may be expressed as

$$X_{str} = \frac{pA}{k} \left(\frac{Lch - \pi R}{2} + R\theta\right) \tag{2.10}$$

where

$X_{str}$ = stretched distance of chain, in.

P = pressure of cylinders, $lb/in^2$.

A = area of cylinder, $in^2$.

K = spring rate, lb.

Lch = total length of chain, in.

Combining equations (2.9) and (2.10) the total expression for piston displacement is

$$X = \frac{Lcy}{2} + R\theta + \frac{PA}{k} \left(\frac{Lch - \pi R}{2} + R\theta\right) \tag{2.11}$$

therefore

$$\frac{dx}{dt} = R\omega + \frac{PAR}{k}\omega + \frac{A}{k} \left(\frac{Lch - \pi R}{2} + R\theta\right)\dot{p} \tag{2.12}$$

where $\omega$ = angular velocity, rad/sec.

Combining equations (2.5), (2.6), (2.7), (2.8), (2.11), and (2.12)

$$q_i = A\left[\left(R + \frac{\rho AR}{k}\right)\omega + \frac{A}{k}\left(\frac{Lch - \pi R}{2} + R\theta\right)\dot{p}\right] + Lp$$

$$+ \frac{A}{\beta}\left[\frac{Lcy}{2} + R\theta + \frac{\rho A}{k}\left(\frac{Lch - \pi R}{2} + R\theta\right)\right]\dot{p}$$

Simplifying

$$\dot{p} = \frac{q_i - A\left(R + \frac{\rho AR}{k}\right)\omega - L_p}{A\left\{\frac{\left(\frac{Lcy}{2} + R\theta\right)}{\beta} + \left(\frac{\rho A}{\beta k} + \frac{A}{k}\right)\left(\frac{Lch - \pi R}{2} + R\theta\right)\right\}} \qquad (2.13)$$

This is the non-linear state variable representation of the derivative of pressure as a function of flow, angular displacement, angular velocity, and pressure. This equation may be implemented directly as it is for a non-linear analysis or may be linearized about some operating point for a linear analysis. If $\theta$ and $\dot{\theta}$ are replaced by $-\theta$ and $-\dot{\theta}$, the equation for piston B results.

Summing moments around the turntable, it is found that

$$T = I\dot{\omega} + f(\omega) = (F_A - F_B)R + M_{ext} \qquad (2.14)$$

where $T$ = total torque, in-lbf.

$I$ = moment of inertia of turntable and load, lbm $in^2$.

$f(\omega)$ = nonlinear moment of bearing, in-lb/rad/sec.

$F_A$ = force exerted on chain by piston A, lbf.

$F_B$ = force exerted on chain by piston B, lbf.

$R$ = pitch radius of sprocket, in.

$M_{ext}$ = External moment applied to turntable, in-lbf.

From this equation the following two dynamic equations may be written

$$\dot{\omega} = \frac{AR(P_A - P_B) + M_{ext} - f(\omega) - k_B\omega}{I} \tag{2.15}$$

$$\dot{\theta} = \omega \tag{2.16}$$

where $k_B$ = viscous bearing moment coefficient, in-lbf/rad/sec.

$f(\omega)$ = nonlinear moment of the preloaded bearing, in-lbf.

The "stiction" of the bearing, due to the static and dynamic sliding characteristics of the valve, may be represented by a function of the form in Figure 11.

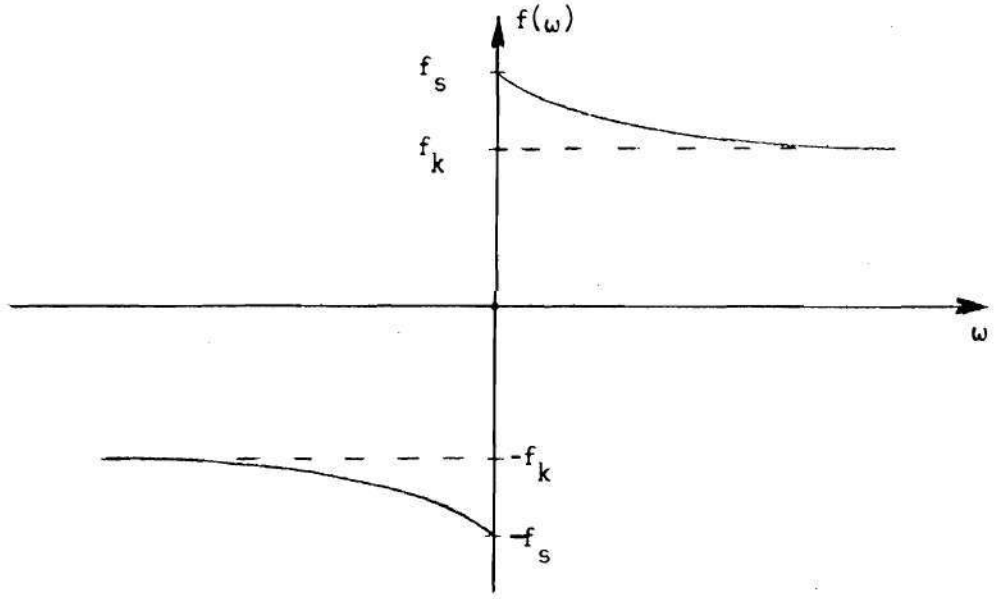


Figure 11. Stiction Moment on Turntable.

where $f_s$ = static friction moment, in-lbf.

$f_k$ = kinetic friction moment, in-lbf.

$\omega$ = angular rate of rotation.

Because of the extremely non-linear characteristics about the origin, a linear representation of this characteristic is impossible. A static moment of 65 ft-lbf and a kinetic moment of 55 ft-lbf were given by the manufacturer. A decaying exponential function of $\omega$ may be used to simulate the function. A convergence rate of $e^{-10\omega}$ was used in this analysis. Equations (2.15) and (2.16) complete the piston-turntable model.

## Hydraulic Lines

The only remaining elements of the system to be modeled are the hydraulic connecting lines between the various system components. There are three major effects on the fluid passing through these lines. A wall resistance results in a net pressure drop across the line. Compressibility of the fluid tends to make the lines act as a capacitor. Finally, fluid mass and inertia serve as an inductive time delay in the response of the line. The most accurate representation of such a resistive, inductive, capactive (RLC) system is a distributed parameter model such as presented by Blackburn (10) as

$$P_b + Z_s Q_b = P_a(t - T_e) + Z_s Q_a(t - T_e)$$

and (2.17)

$$P_a - Z_s Q_b = P_b(t - T_e) - Z_s Q_b(t - T_e)$$

where $P_a$ and $P_b$ = upstream and downstream pressure respectively, $lb/in^2$.

$Q_a$ and $Q_b$ = upstream and downstream volumetric flow rates, respectively, $in^3/sec$.

$t$ = time

$T_e$ = wave travel time along pipe, sec.

$Z_s$ = characteristic impedance of the pipe, $\frac{\text{sec-lbf}}{\text{in}^5}$ .

Here

$$T_e = \frac{\ell}{\sqrt{\beta/\rho}} \approx .001 \text{ sec.}$$

and

$$Z_s = \sqrt{\rho\beta/A^2} \approx 5340 \text{ lbf-sec/in}^5$$

if $\ell$ = 60 in, A = .0625 $\text{in}^2$, $\rho = .78 \times 10^{-4}$ $\text{lbf-sec}^2/\text{in}^4$, $\beta = 270{,}000$ $\text{lb/in}^2$.

If $T_e$ is small in comparison with the significant wavelengths of the system, the distributed parameter representation may be replaced by a much simpler lumped parameter model. In the lumped model, each of the three components of line dynamics, resistance, capacitance, and inertiance, can be modeled separately and combined to simulate the entire line. The order in which these pieces may be combined depends upon the particular input and output values desired. Because the three components are different, the model can not be symmetrical and will thus not have exactly the same dynamics for one end as for the other. The error incurred here is small and is often necessary to attain a low order model. As described by Blackburn (11), the relationship governing fluid inertance is

$$P_a - P_b = \frac{\ell}{Ag} = I_L \, dw/dt \qquad (2.18)$$

where $P_a$ and $P_b$ = the upstream and downstream pressure respectively, $\text{lb/in}^2$.

$\ell$ = line length

A = cross sectional area of the pipe, $\text{in}^2$.

$g$ = acceleration of gravity, $ft/sec^2$.

$W$ = weight rate of flow, $lb/sec$.

$I_L$ = line inertance, $sec^2/in^2$.

Fluid capacitance is given as

$$\omega_a - \omega_b = \frac{\gamma A \ell}{\beta} \, dP/dt = C_L \, dP/dt \qquad (2.19)$$

where the terms not already defined are

$\gamma$ = specific weight of fluid, $lb/in^3$.

$\beta$ = fluid bulk modulus, $lb/in^2$.

$C_L$ = line capacitance, $in^2$.

Finally, fluid resistance, a nonlinear quantity when the flow is turbulent and a linear term when the flow is laminar, can be approximated by the relationship

$$\Delta P = C_\ell \, \rho/2 \, |V_L| V_L = R_L W \qquad (2.20)$$

where $\rho$ = fluid density, $lbm/in^3$.

$V_L$ = fluid velocity, $in/sec$.

$C_\ell$ = loss coefficient.

$R_L$ = fluid resistance, $sec/in^2$.

A block diagram representation of each of the three components is shown in Figure 12.

The particular line model to be used will not be chosen here, but will be chosen when the type of model needed has been established. At this point, all of the elements of the system have been modeled.

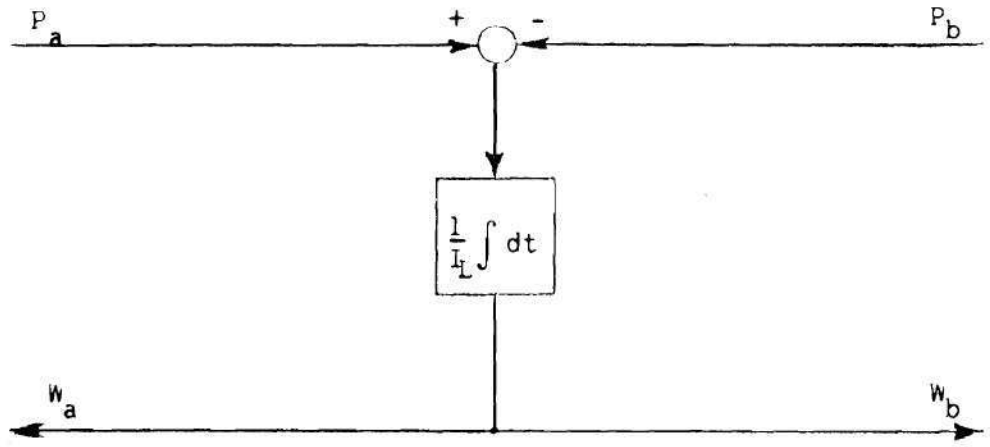


a) Inertance

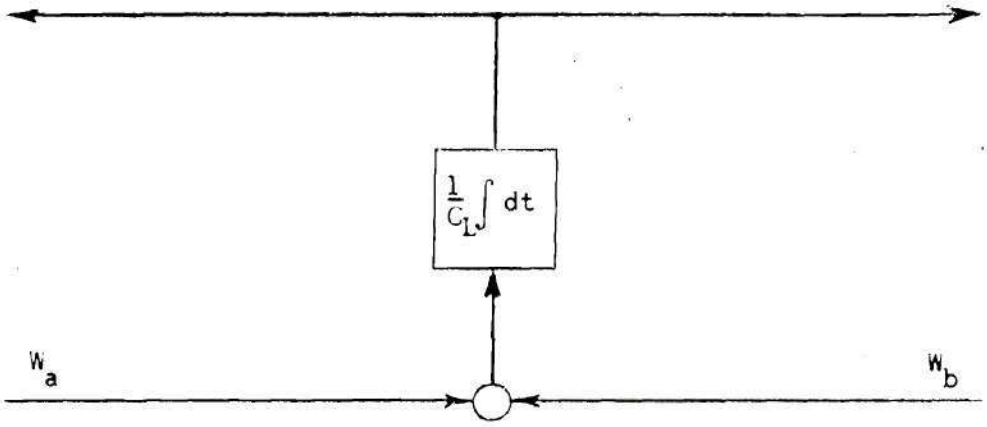


b) Capacitance

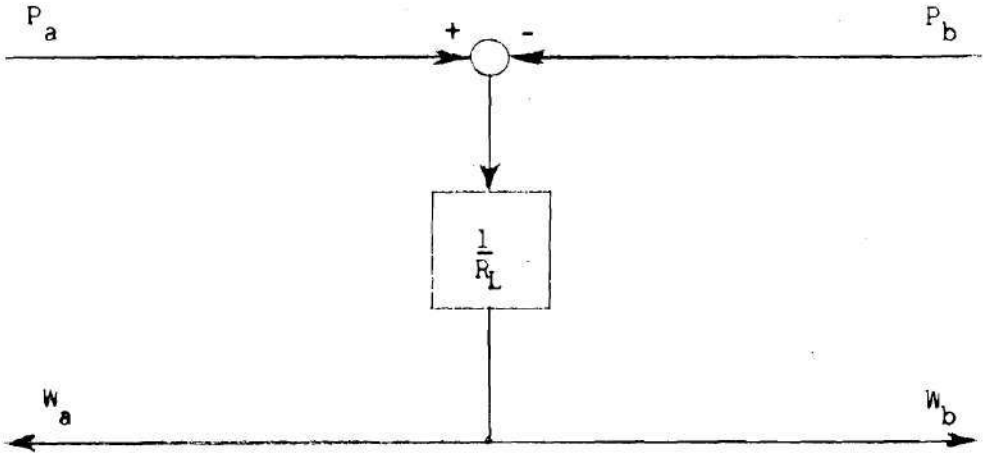


c) Resistance

Figure 12. Block Diagrams of Fluid Elements.

# CHAPTER III

## IMPLEMENTATION OF THE MATHEMATICAL MODEL

Having completed the basic mathematical representation of the dynamics of each of the system components, the next task is the unifying of these individual pieces into a system. Both a linear and a non-linear system of equations are developed. First, a linear model is developed through a series of tests made to determine the performance limits of the hardware. Using the linear model as a base, the non-linear model is systematically built. As each non-linear effect has been added, its effect on the system has been analyzed.

The reason for developing both a linear and a non-linear model is twofold. The development of the linear equations and the implementation of these equations in a numerical simulation is generally more simple than developing and implementing the corresponding non-linear system. If in fact the linear model were to give results of sufficient accuracy, much work and computational time could be saved. On the other hand, without a non-linear model, the significance of certain non-linear characteristics may never be determined.

A fourth-order Runge-Kutta integration scheme is used in both system models to simulate the system in time. State variable techniques are utilized (12). The integration, essentially a numerical boundary value "shooting" (13) technique, constructs the paths in state space of the state variables as functions of time. Although this is a discrete

approximation technique, very accurate results are possible if a sufficiently small integration step size is used.

The linear representation of the control system consists of the linearized versions of each of the component models. The controller and servovalve can be represented simply by the transfer functions of equation (2.1) and Figure 5. The transfer function for the pistons, equation (2.13), is highly non-linear. Therefore, a linearization of this equation about some operating point yields the following linear relation for $\dot{p}$

$$\dot{p} = \frac{q - (L + k5)p - k1\omega - k6\theta + k7}{k4} \qquad (3.1)$$

where $k1 = Ak\left(1 + \frac{p_o A}{k}\right)$

$$k2 = \left(\frac{Lch - \pi R}{2} + \theta_o R\right)$$

$$k3 = q_o - Lp_o - k_1\omega_o$$

$$k4 = A^2/\beta\left\{\frac{1}{k}(\beta + p_o)k_2 + 1/A\,(Lcy/2 + R\theta_o)\right\}$$

$$k5 = \frac{A^2/k\left(k4\,R\omega_o + \frac{k3k2}{\beta}\right)}{k4}$$

$$k6 = \frac{A^2 Rk3}{\beta k4}\left(\left(\frac{\beta + p_o}{k}\right) + 1/A\right)$$

$$k7 = k5p_o + k6\theta_o$$

where $A$ = piston area, $in^2$.

$R$ = pitch radius of sprocket, in.

$k$ = spring rate of chain, lb.

$Lch$ = length of the chain, in.

$Lcy$ = length of cylinder, in.

$\beta$ = bulk modulus of fluid, $lb/in^2$.

L = leakage coefficient, $in^3/sec/lb/in^2$.

q = flow into cylinder, $in^3/sec$.

p = pressure of cylinder, $lb/in^2$.

$\theta$ = angular displacement of turntable, radians.

$\omega$ = angular velocity of turntable, radians/sec.

Note that to calculate $\dot{p}$ for piston B (see Figure 10) q, $\theta$, and $\omega$ must change sign. This represents the linearized pressure derivative of the cylinder.

The remaining elements of the system are the turntable-chain combination and the line dynamics. With the exception of the bearing friction, all of the elements of the turntable-chain combination which were not incorporated in the above relation for $\dot{p}$ are linear. Unfortunately, because of the unusual shape of the function (see Figure 10), no linear model of this effect is possible. Some viscous friction may still be present, however, and this factor is included in the model. At this point, line dynamic effects are assumed negligible and are not included. This assumption will be validated after a few time constants of the system have been established. Since the time constant of the controller is of the same order as the time delay (.001 sec), the controller dynamics are also neglected and a constant gain is assumed for the controller. A block diagram of the entire linear configuration may be seen in Figure 13.

Once the linear model is working correctly, several parameters of the system are changed to determine which were the most critical to the analysis. The parameters varied are servocontroller gain, inertia of the turntable and load, viscous bearing friction, and leakage of the piston.

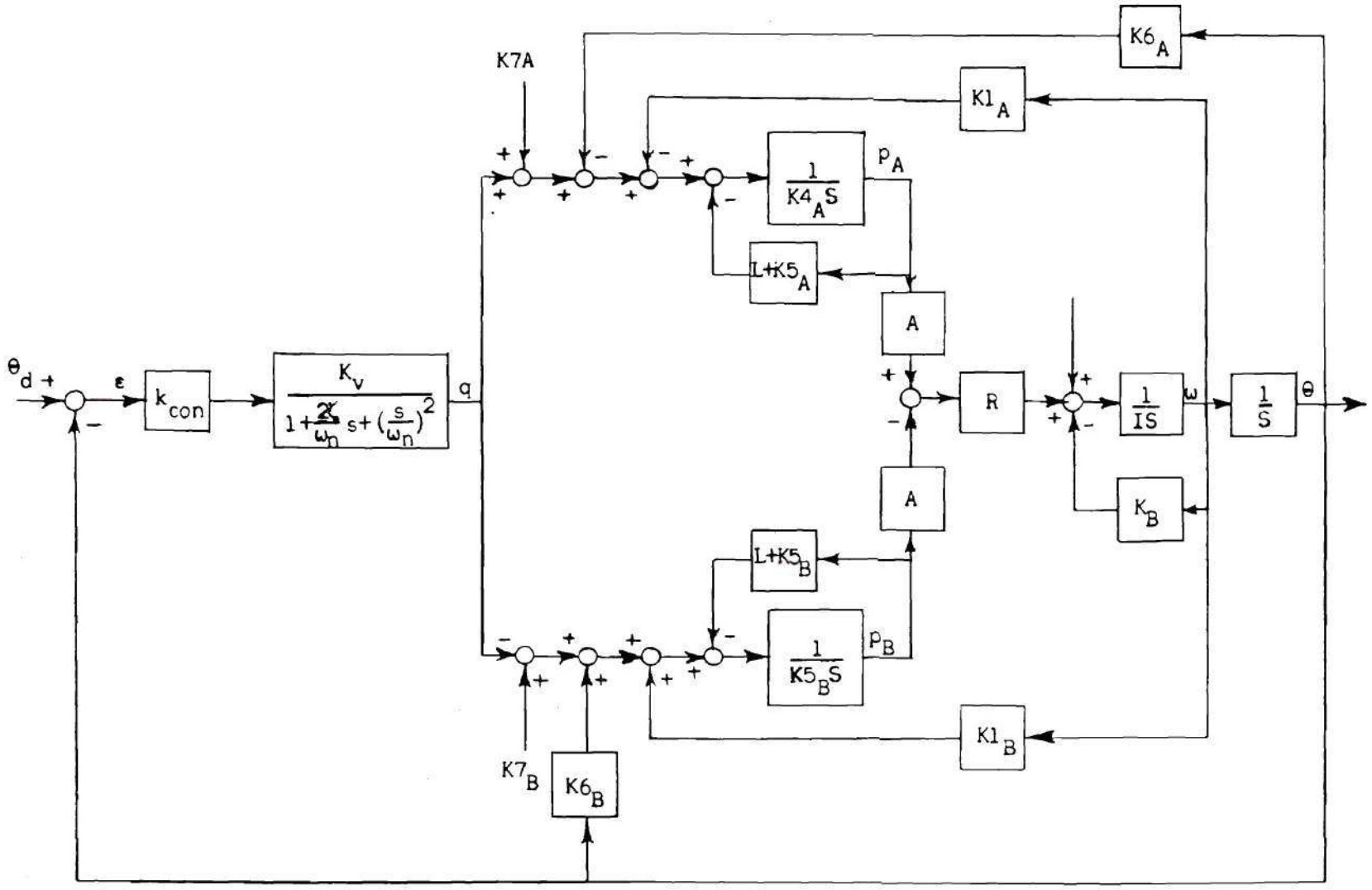


Figure 13. Block Diagram of Linear Model of Hydraulic System.

The results of each variation will be discussed individually and conclusions will be made. A variation in one parameter will not be as meaningful unless all remaining parameters are constant throughout the test. Therefore, each parameter is varied individually. The nominal values for the parameters which will be varied are given as

| | |
|---|---|
| Amplifier Gain | 6000 ma/radian |
| Turntable and Load Inertia | 50,000 lbm - $in^2$ |
| Bearing Viscous Friction | $7.7 \times 10^{-4}$ in-lb/radian/sec |
| Leakage Coefficient | $1 \times 10^{-6}$ $in^3$/sec/lb/$in^2$ |

The amplifier gain was chosen to give good system performance. The inertia was a representative load as given by the manufacturer. The viscous friction coefficient and the leakage coefficient were crude estimates of factors which will later be shown to have little effect on the system if these factors are chosen reasonably.

Plots of the system response to a step input from a finite displacement to zero displacement for various values of controller gain are given in Figure 14. In this figure and the remaining parameter variation curves, pressure in cylinder A (see Figure 10) and turntable displacement are given. Only two pressure curves are given because the data tended to overlap and become indistinguishible if all data was presented. It may be seen from Figure 14 that as gain increases, response time decreases, but at the cost of system oscillation about the target. As gains approach 100,000 ma/radian, the system becomes unstable. At a gain of 45,000 ma/radian the fundamental frequency of pressure oscillation is a clearly visible characteristic frequency of the displacement.

The higher frequency vibration, noticeable in the pressure graph

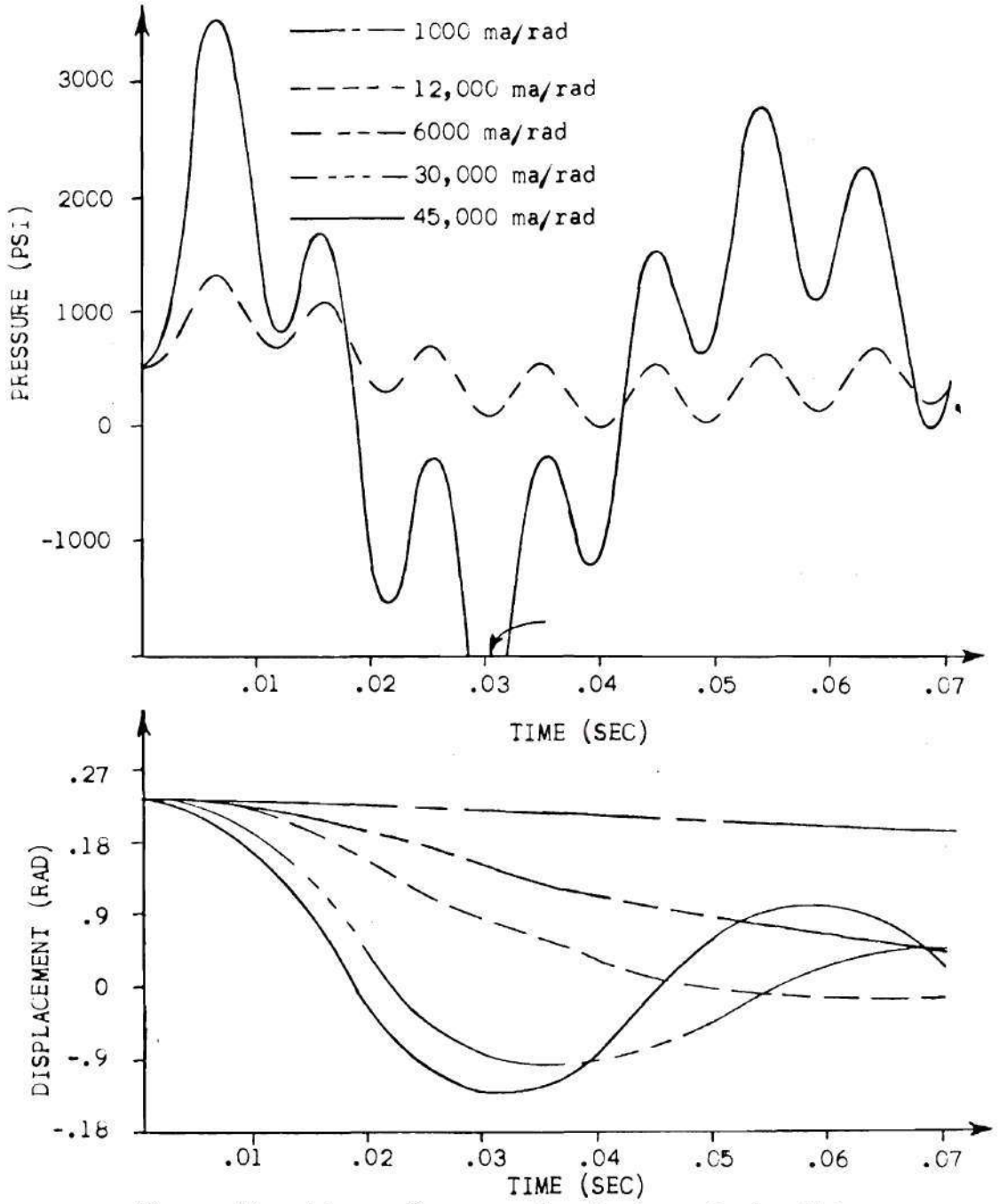


Figure 14. Linear Response for Various System Gains.

of Figure 15 is not due to the gain of the system, but is rather an effect of the inertia of the turntable and load. The cylinder pressures of Figure 3.3 have a frequency which decreases as inertia increases. That is, for an inertia of 2300 lbm-in$^2$, the force required to initiate movement of the turntable is small. Hence, an oscillation too small to be visible in this graph is present in the pressure curve. As inertia increases, pressure peaks and the wavelengths of this oscillation each increase. Hence, the period of oscillation of the system with a 100,000 lbm-in$^2$ inertia, .0138 sec., is longer than that of the smaller, 50,000 lbm-in$^2$ inertia, .009 sec. Because these pressure oscillations are at a relatively high frequency, they are not generally observable in the displacement of the turntable. For such extremely large amplitude and low frequency oscillations as the 1,000,000 lbm-in$^2$ case, the frequency of oscillation may be seen in a low amplitude oscillation about the path toward the target.

An examination can be made here of the validity of neglecting line dynamics. Of the six hydraulic lines of the system, only four carry fluid under compression. The two lines from the pistons to the reservoir are used simply to return the leakage flow of the piston to the reservoir. Of the remaining lines, the longest are between the valve and cylinders. These two lines thus have the longest delay time and the greatest likelihood of affecting the system.

A line delay time of .001 sec. has an equivalent natural frequency of 1,000 radians/sec. The highest frequency observable in the nominal parameter model (50,000 lbm-in$^2$ load) is approximately 100 cycles/sec of 628 radians/sec. Although a strong argument could be made for its

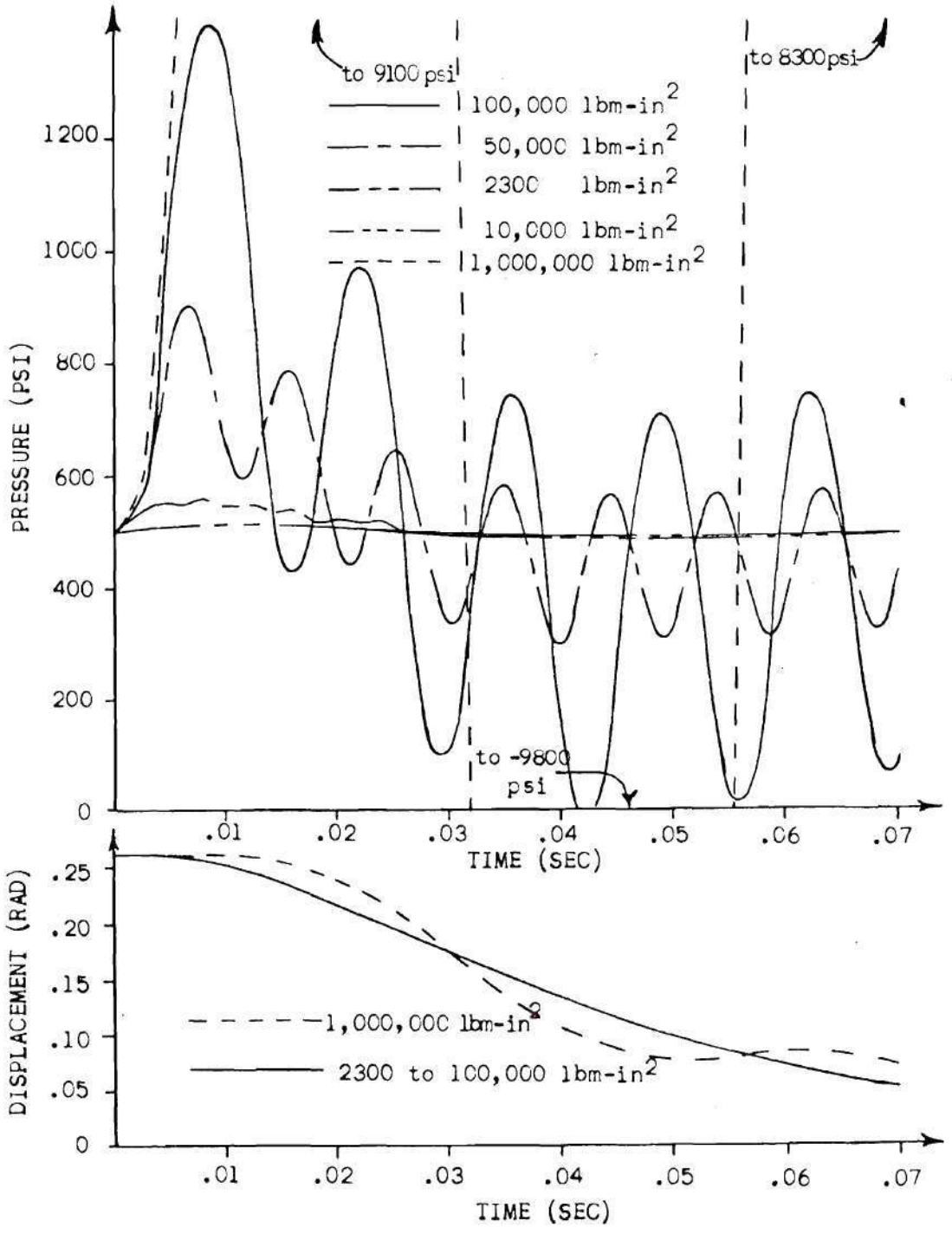


Figure 15. Linear System Response for Various Inertias.

inclusion, the addition of these two lines to the non-linear model would have increased the order of the complete system from six to ten. The added accuracy of the inclusion of this effect was sacrificed for simplicity of the model and a savings of computation time. Any further analysis broadening the scope of consideration of this model would surely find line dynamics among the first factors to consider.

Observing the oscillatory motion of the pressure, the reason for this phenomenon becomes an obvious question. Since the frequency increases as the mass decreases, the system is obviously responding as a spring-mass combination. The two possible sources for the spring effect are the hydraulic spring of the fluid under compression and the mechanical spring of the chain. Figure 16, similar to the pressure graph of Figure 15, includes curves representing the effect of the volume of fluid under compression and the length of chain subject to stretching being individually doubled. Since volume change and chain length change each visibly alter the original graph, each component is necessary and significant in the model.

Variation in bearing friction gives an extremely interesting result. Figure 17 depicts the changes in pressure and angular displacement with bearing friction. As may be seen in the graph, the damping of the spring-mass oscillation increases dramatically as the viscous friction reaches high levels. The major benefit of this phenomenon is the reduction in system fatigue by eliminating a substantial amount of the pressure variation. A problem with regard to this rather advantageous characteristic is the large viscous friction coefficient necessary to achieve this damping (13,000 in-lbm/rad/sec).

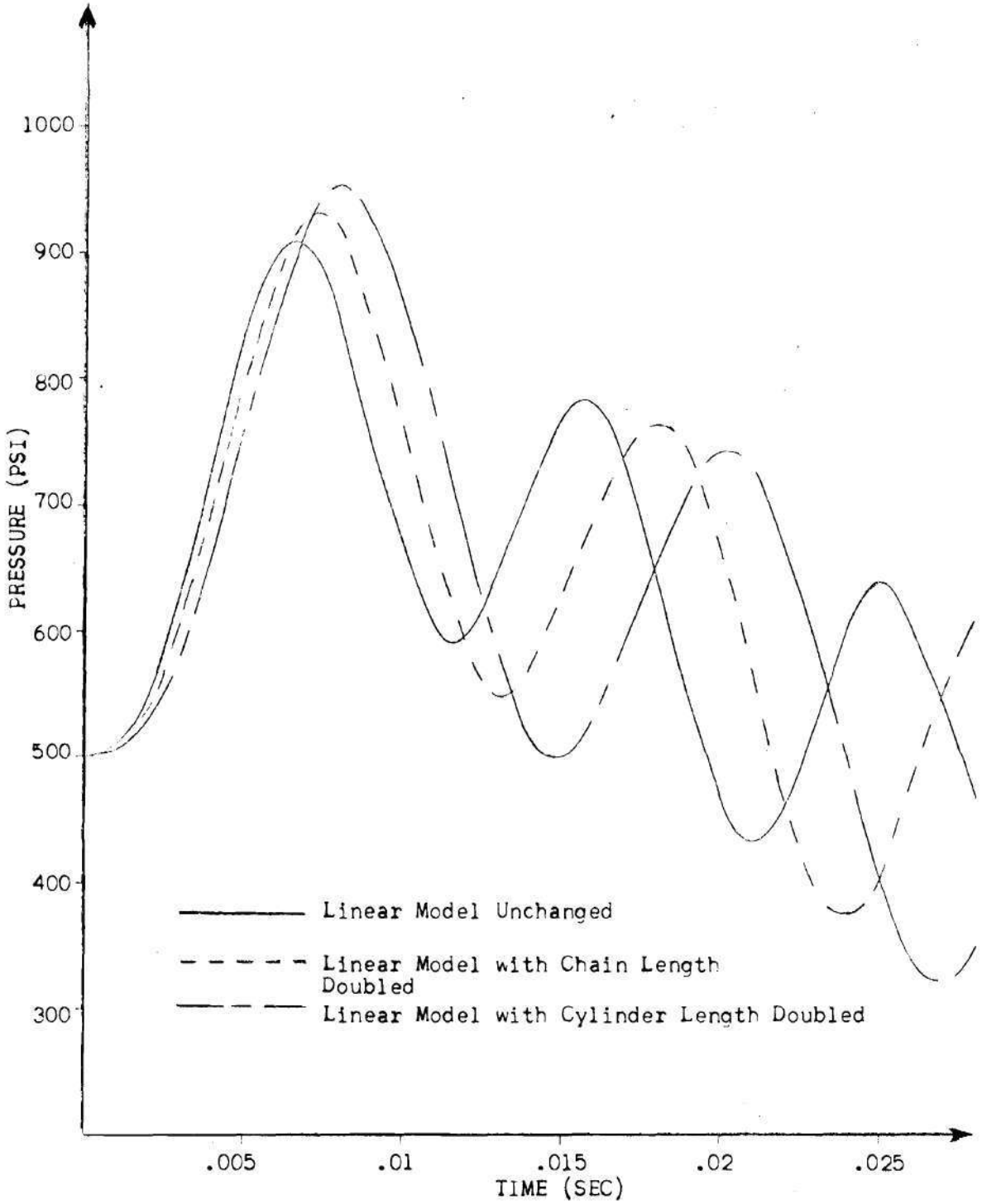


Figure 16. Linear System Response with Variation in Cylinder and Chain Length.

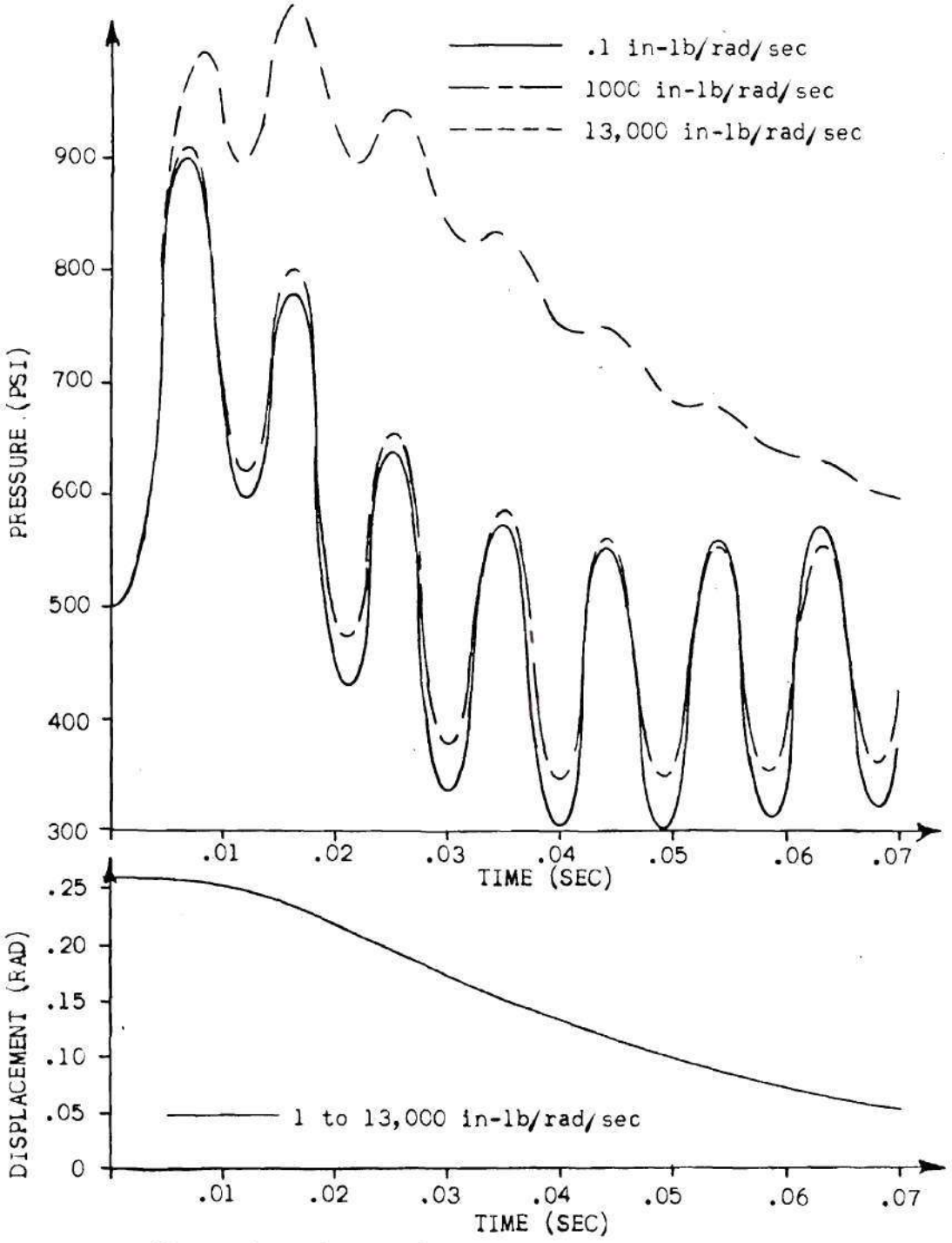


Figure 17. Linear Response for Various Viscous Bearing Friction Coefficients.

The final parameter to be varied is the piston leakage coefficient. A potential advantage of increasing the leakage could be a reduction in peak values of pressure or an increase in damping of those oscillations. As can be seen in Figure 18, the reduction in pressure peaks was relatively small. Essentially no change in performance loss can be seen in the angular displacement curve as leakage is increased for $10^{-6}$ to $10^{-3}$ $in^3/sec/lb/in^2$. Although a slight increase in damping can be achieved, the cost associated with this damping (.5 $in^3/sec$ leakage at 500 psi) is extremely high.

Once the linear testing was completed, the creation of the non-linear model remained. Each non-linearity was added individually to attempt to identify the most critical non-linear factors. The actual computer methods involved in the implementation of the non-linearities may be found in Appendix B.

In sequential order, the non-linearities due to the calculation of $\dot{p}$ (Equation (2.13)), the square root orifice law of the valves, and the stiction of the turntable assembly were added. Their effects on pressure and angular displacement are presented in Figures 19 and 20. As may be seen in the wide difference between the model including stiction and the others, this stiction seems to be the only effect which causes the system to vary significantly from the linear model. This may be expected since stiction is not included in the linear analysis.

The effect of adding the final non-linearity, saturation, may be seen in Figure 21. The nonlinear model is in its final state at this point. In this figure, saturation has caused the system to respond in a much more inhibited way than the linear model to a step input. Again,

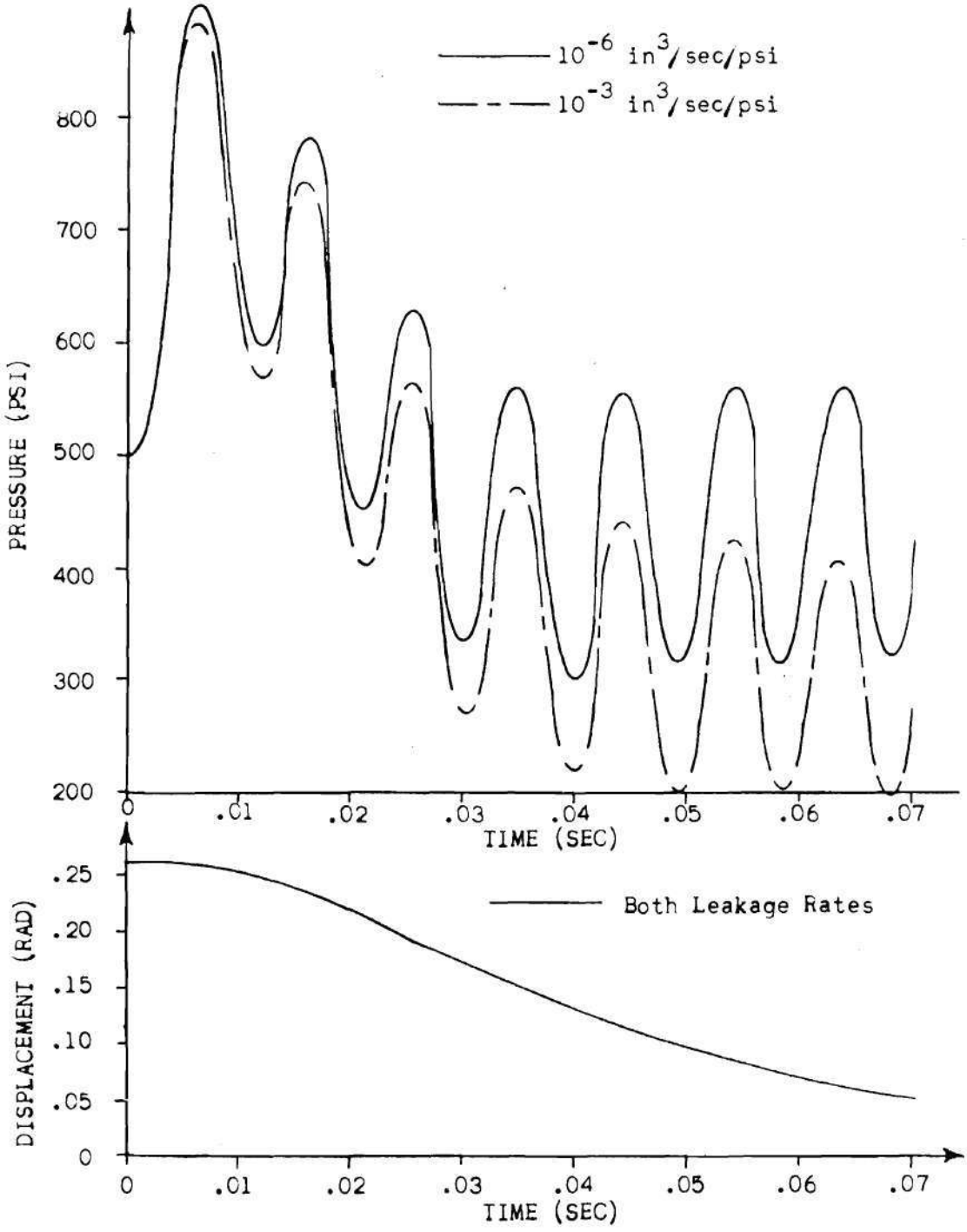


Figure 18. Linear Step Response for Various Leakage Coefficients.

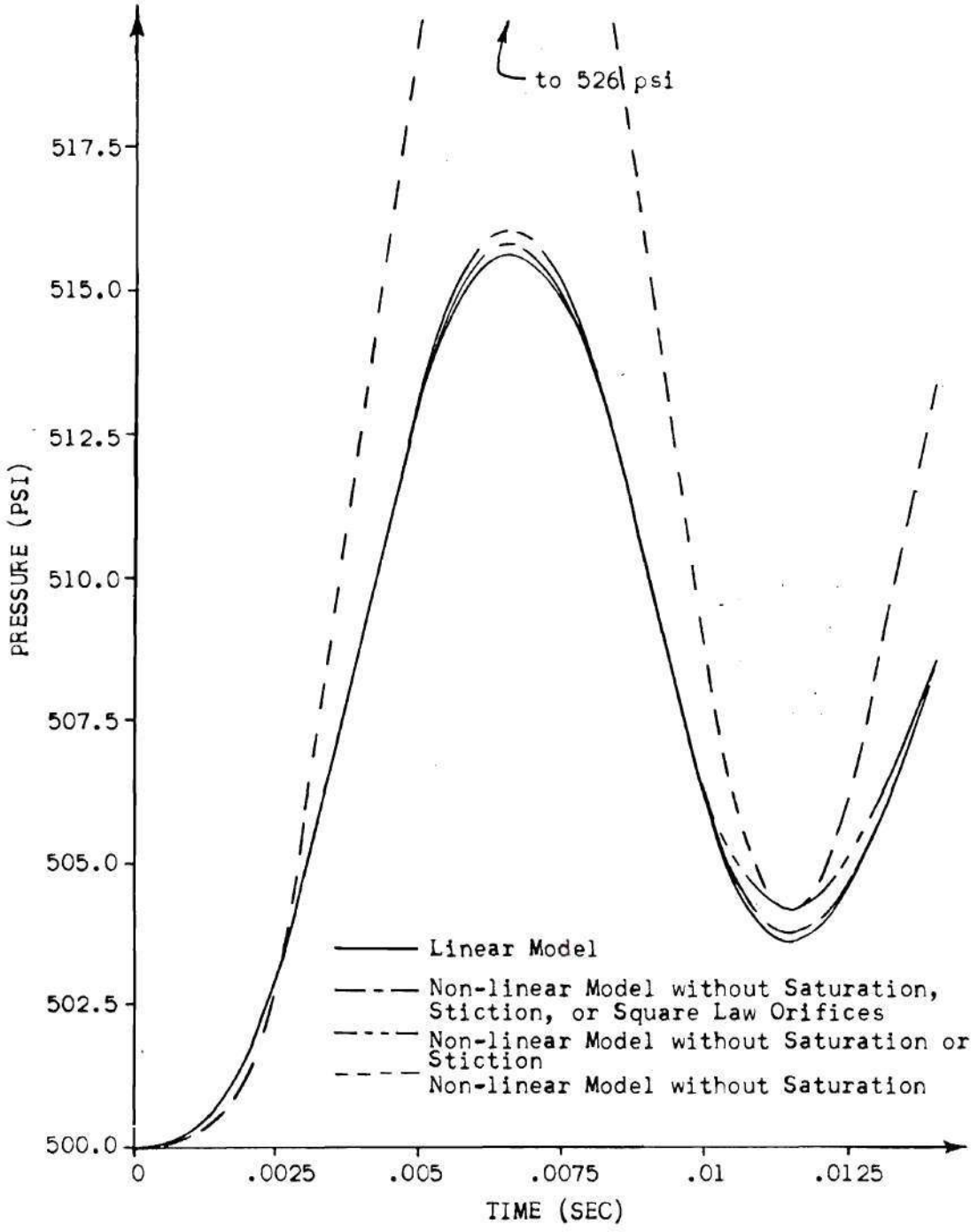


Figure 19. Pressure Step Response of Linear and Various Non-linear Models.

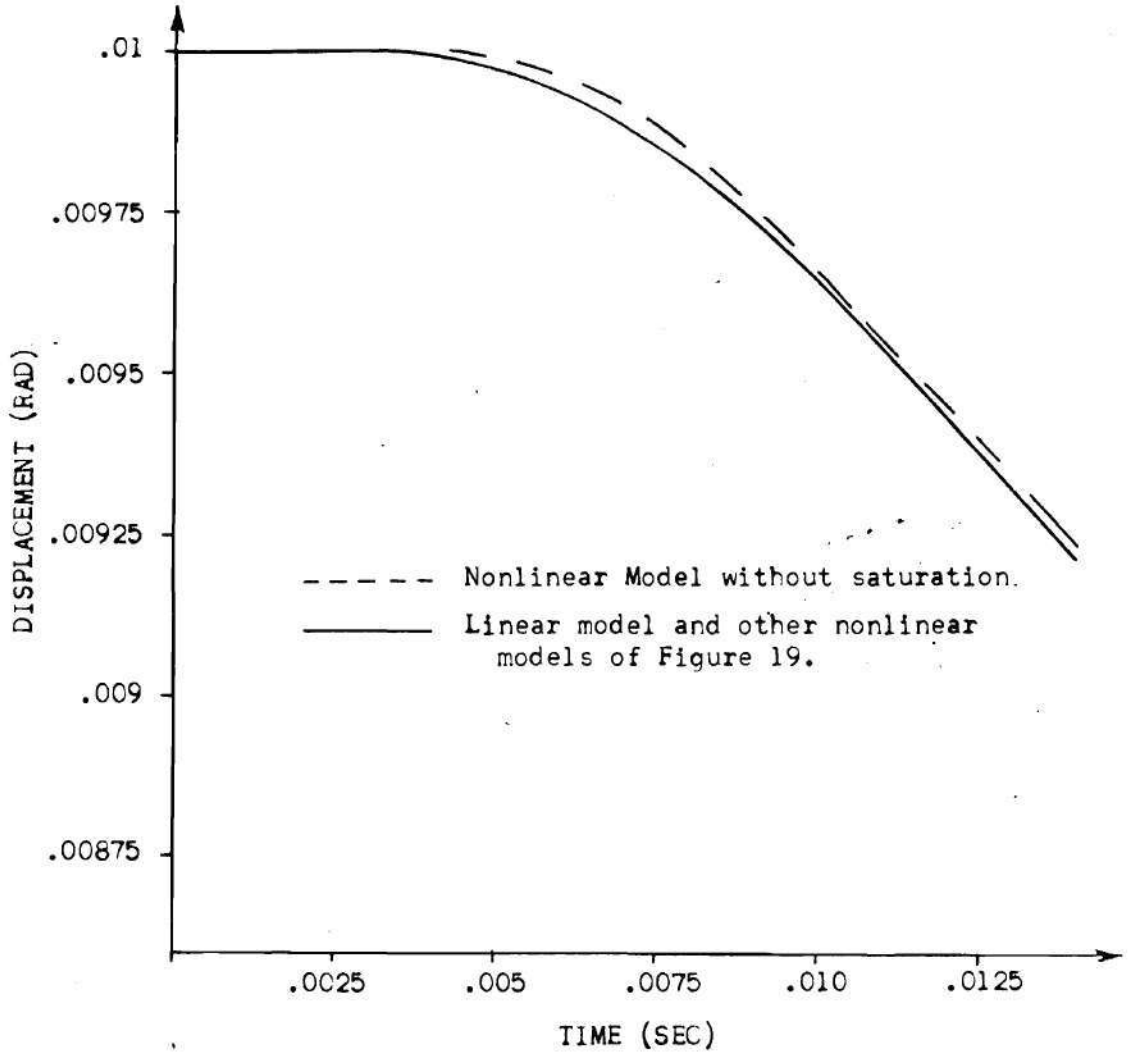


Figure 20. Displacement Step Response of Linear and Various Non-linear Models.

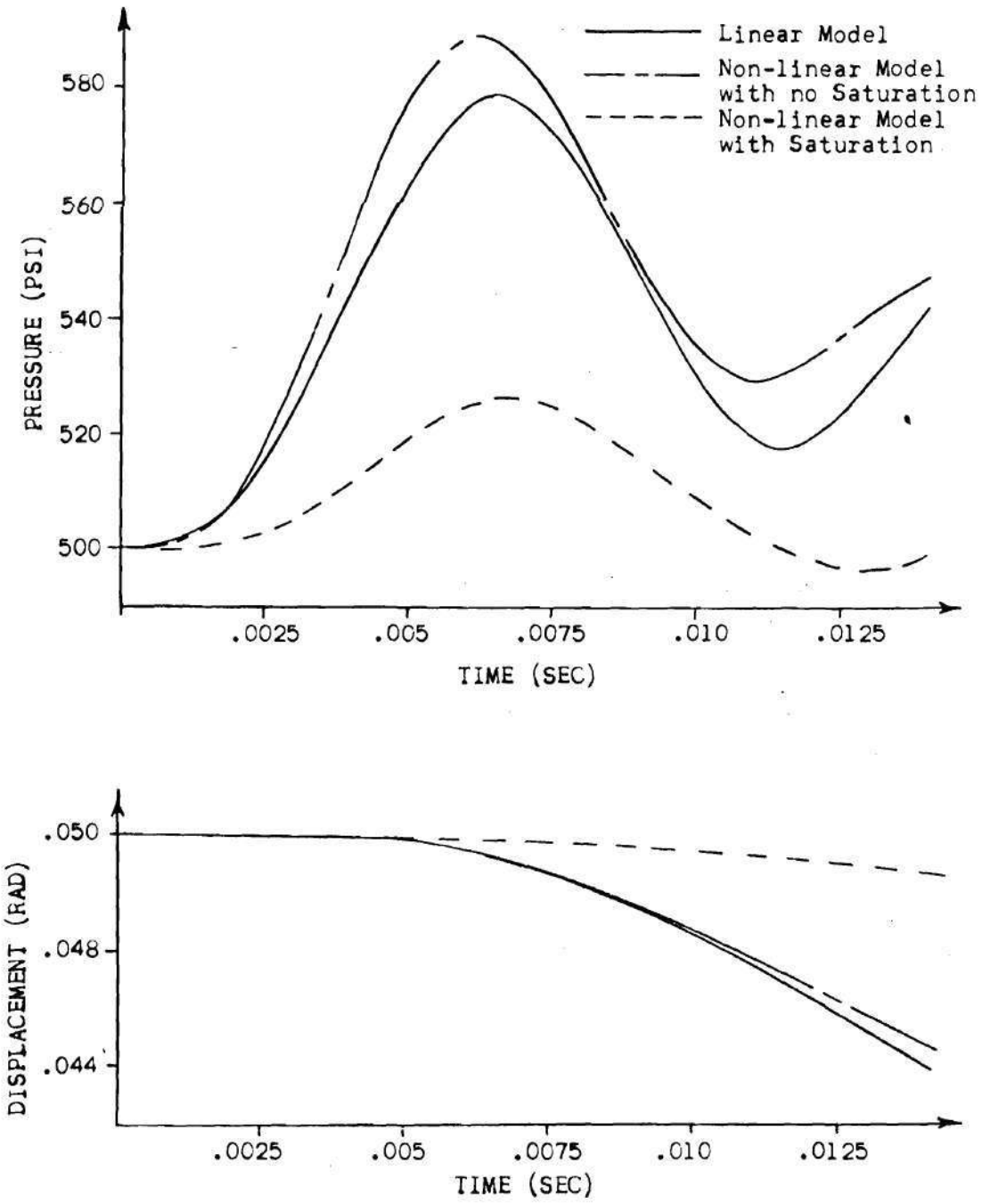


Figure 21. Response of Linear and Non-linear Models to a Small Step Input.

the shape of the pressure curves are similar, but of different magnitudes.

When the input step is increased, from .05 to .2 radians, the shape of non-linear model makes a radical departure from that of the linear model. This difference is most evident in the non-linear model in which no saturation is considered. As can be seen in Figure 22, this model no longer experiences the oscillatory motion of the linear system, but quickly damps out this tendency. Investigating this apparent damping phenomenon further, a graph depicting the pressure of the cylinder for a series of larger and larger input steps is shown in Figure 23. The steadily increasing damping of the systems may be best explained by examination of a different linear model with a slightly altered configuration.

If a leakage is induced between the ends of the piston connected to the valve, the pressure curves of Figure 24 result. The curves of this figure indicate that an effect similar to the non-linear damping may be realized by allowing this leakage flow between the pistons.

From the above observations, a conclusion may be reached as to the explanation of this damping of the non-linear model. In Figure 25, the linear and non-linear pressure-flow relationships are show for various spool displacements. As may be seen, the linear approximation significantly overestimates the actual flow through the valve for high spool displacements. A reduction in flow equal to the difference between the linear and non-linear flow curves has been induced by the leakage between the pistons. To reduce the flow at the first pressure peak of the linear model that predicted by the non-linear model, a flow coefficient of

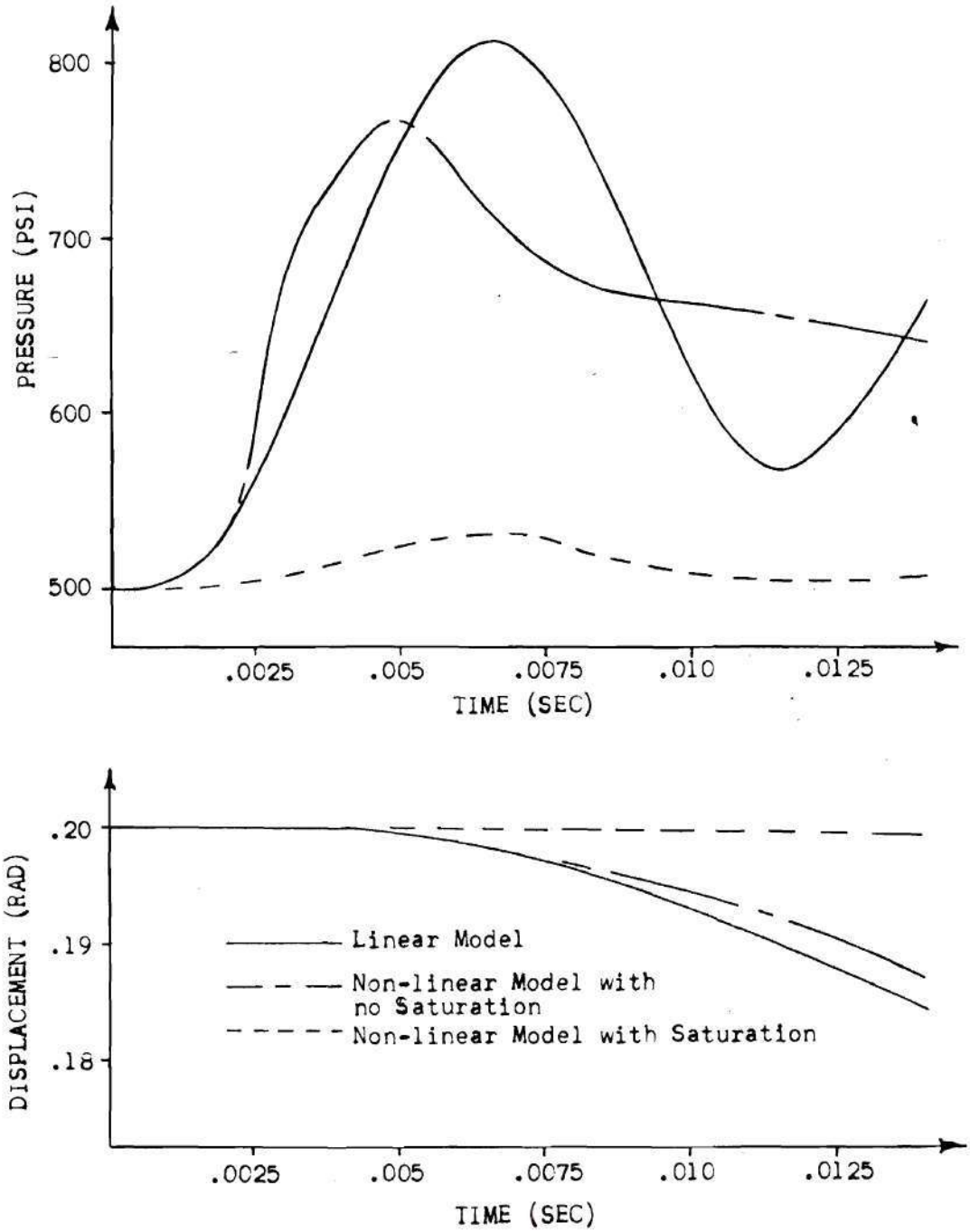


Figure 22. Response of Linear and Non-linear Models to a Large Step Input.

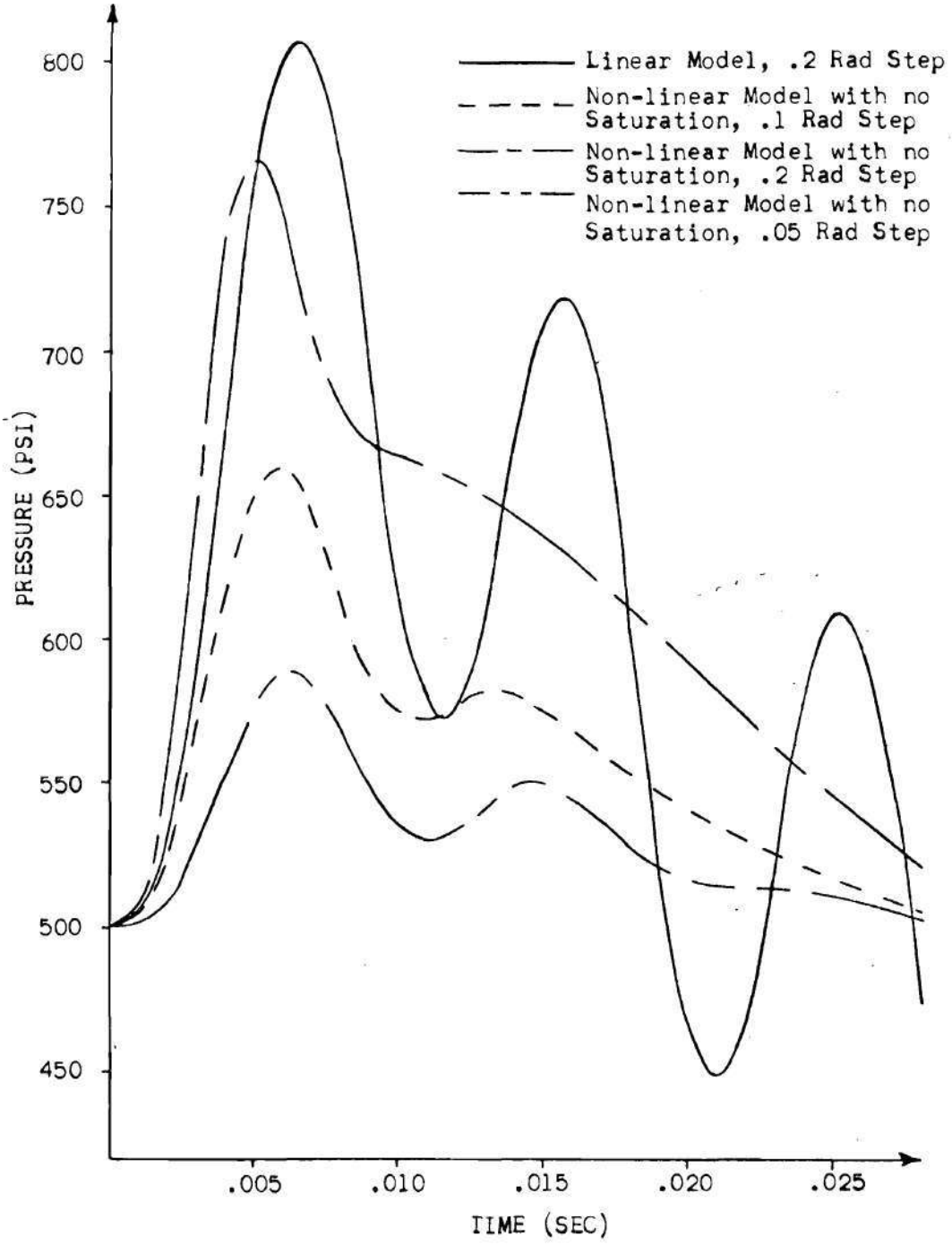


Figure 23. Pressure Response of Various Models for Different Step Inputs.

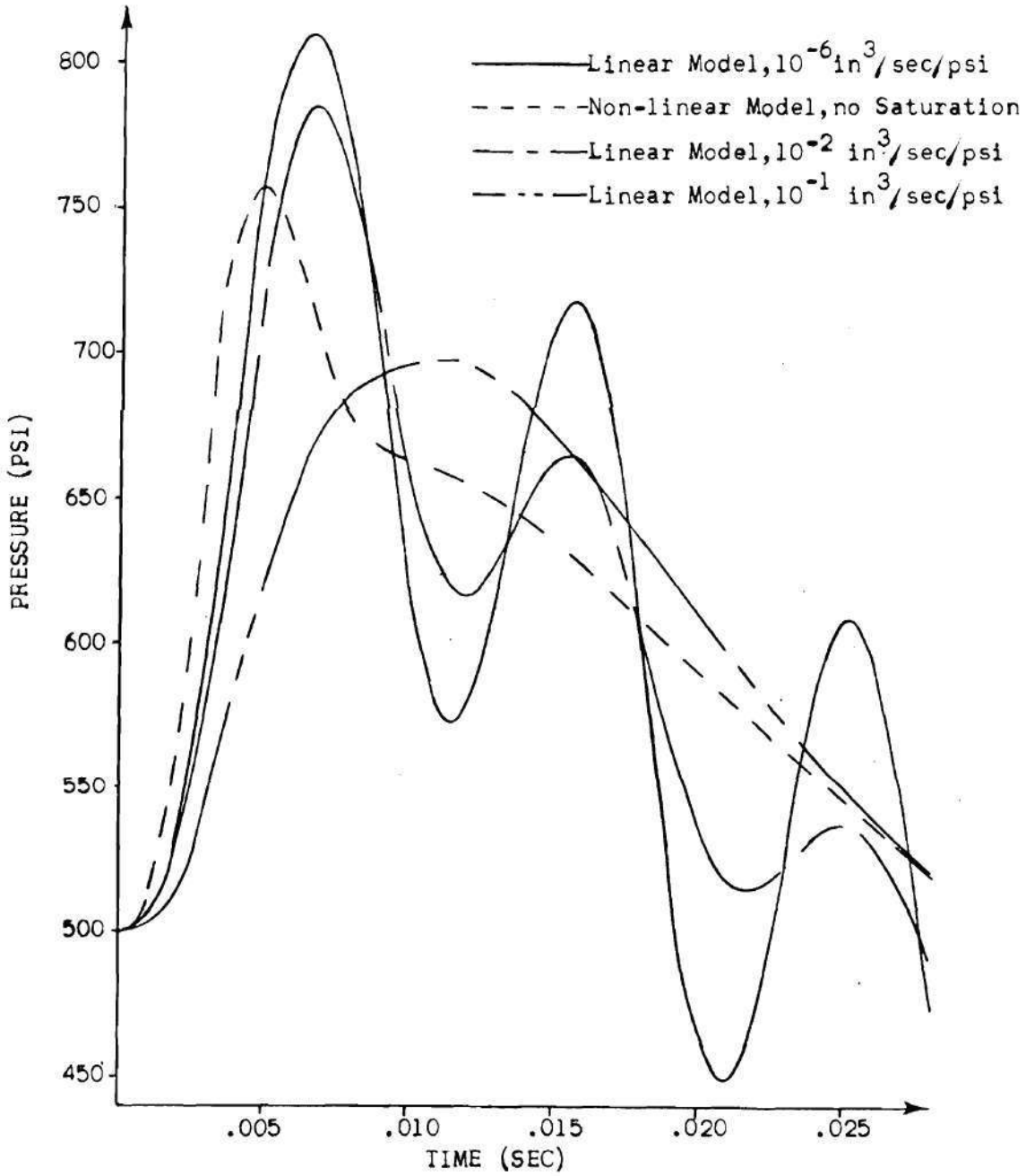


Figure 24. Pressure Step Response of Linear Model for Several Leakage Coefficients Between Pistons.

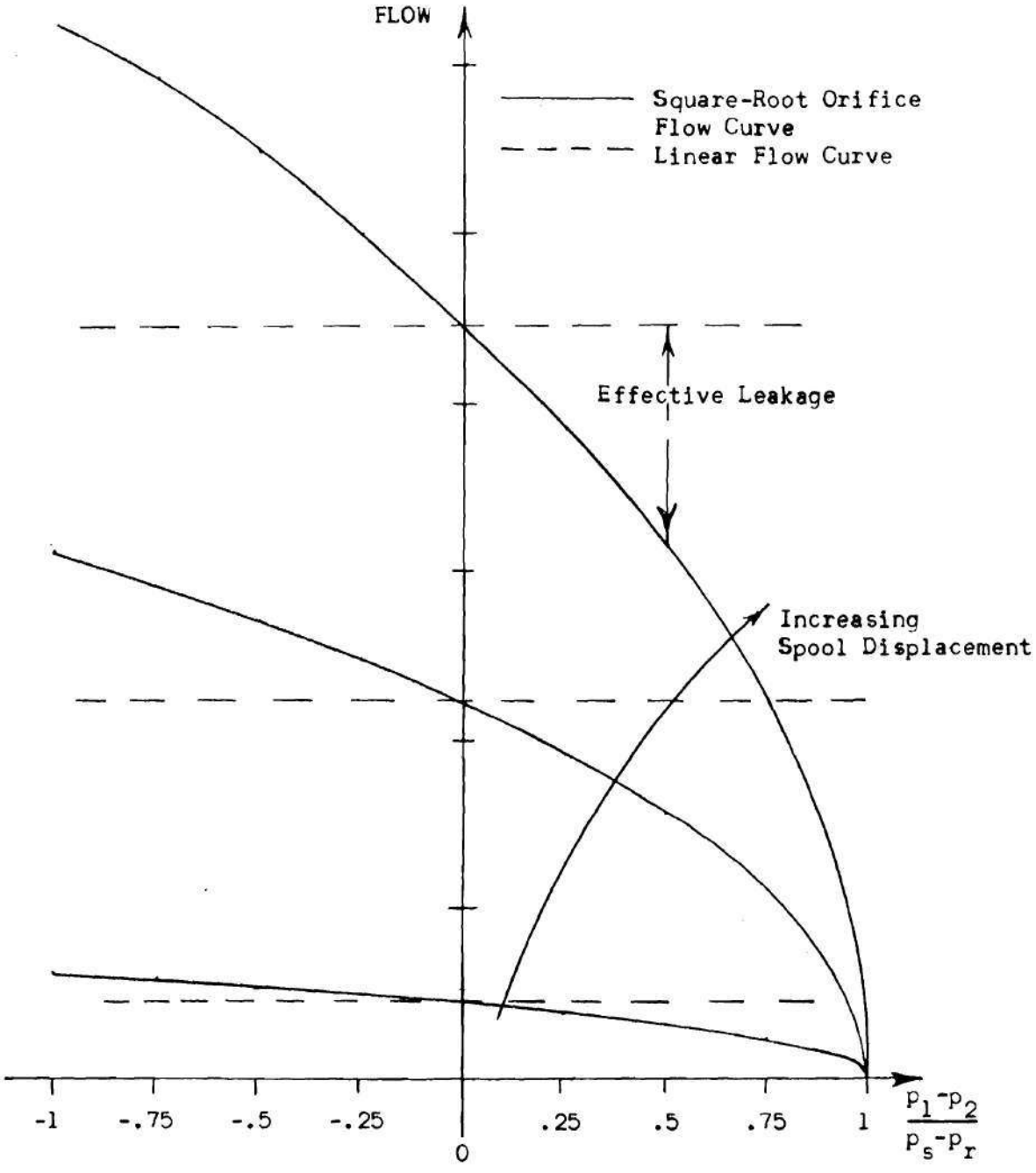


Figure 25. Linear and Non-linear Flow Curves for Various Spool Displacements

approximately .1 $in^3/sec/lb/in^2$ is required. The similarity of curves supports the above explanation of this phenomenon.

This modification of the linear model indicates a method to simulate the pressure damping of the non-linear model, but cannot be used in general because the degree of flow variaties due to this effect is a function of spool displacement. The non-linear model including saturation still tends to oscillate at the same frequency and amplitude as the smaller step. This is due to the fact that saturation has completely determined the motion in both cases. From Figures 21 and 22, it becomes quite clear that saturation has a tremendous impact on the response of the system.

A long time response of the system may be seen in Figures 26 and 27 in which pressure and angular displacement are given for a comparatively long time interval. The major observations to be made are the slower response of the saturated non-linear system and the lack of significant damping of the pressure oscillations in the linear model. The final values for the displacements are of extremely small amplitude. The discontinuous nature of the bearing friction model tends to artificially force the turntable to shift repeatedly from positive to negative. This jumping about is reduced when saturation is induced into the model by removing the very rapid responses. This effect is minor and is not found in the actual hardware.

The testing of the actual positioner was carried out at Scientific-Atlanta on two positioners assembled there. One of these may be seen in Figure 1. Each positioner was subjected to a series of tests. The monitoring equipment consisted of a two channel brush recorder capable of

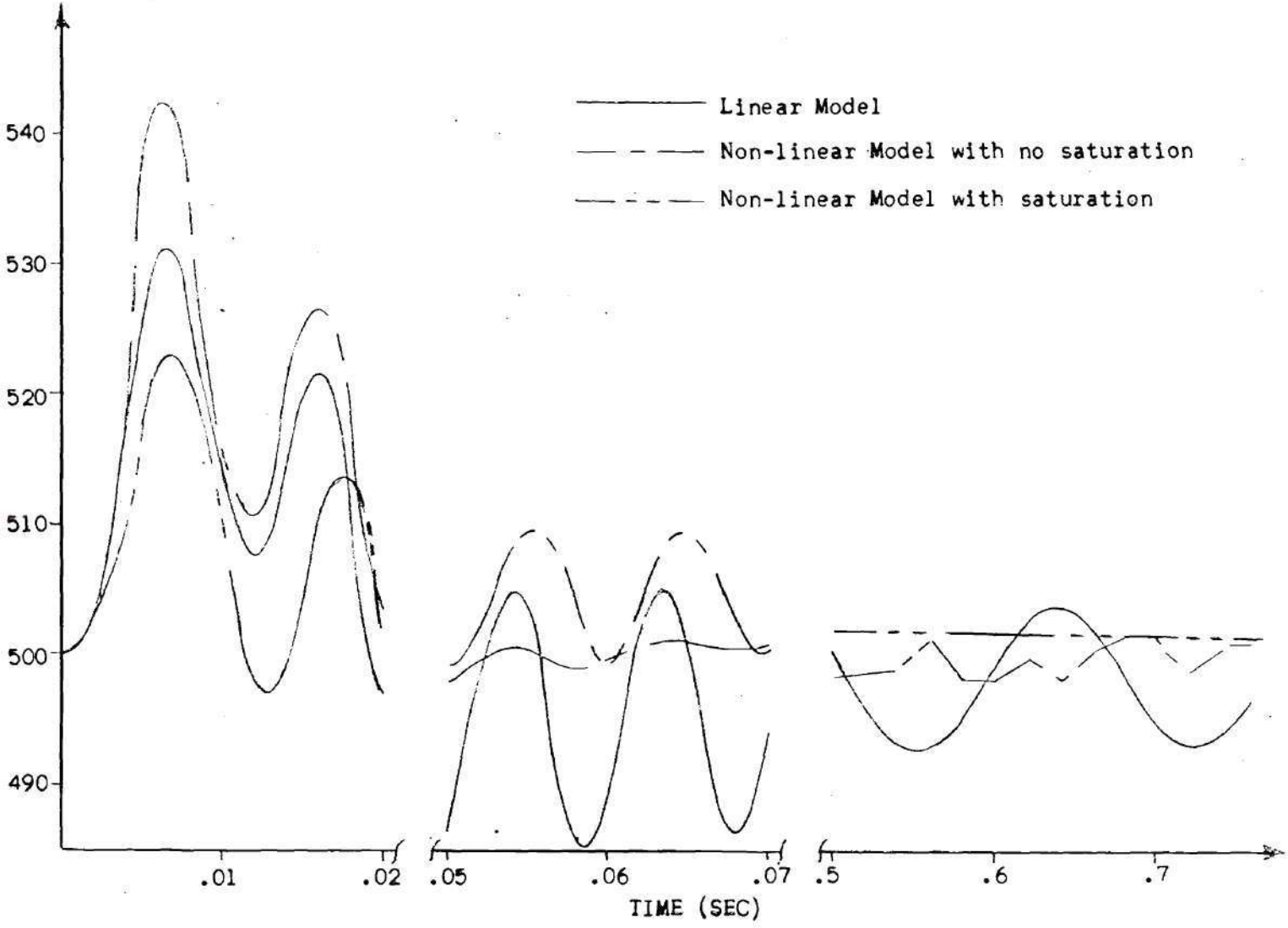


Figure 26. Cylinder Pressure for Various Models.

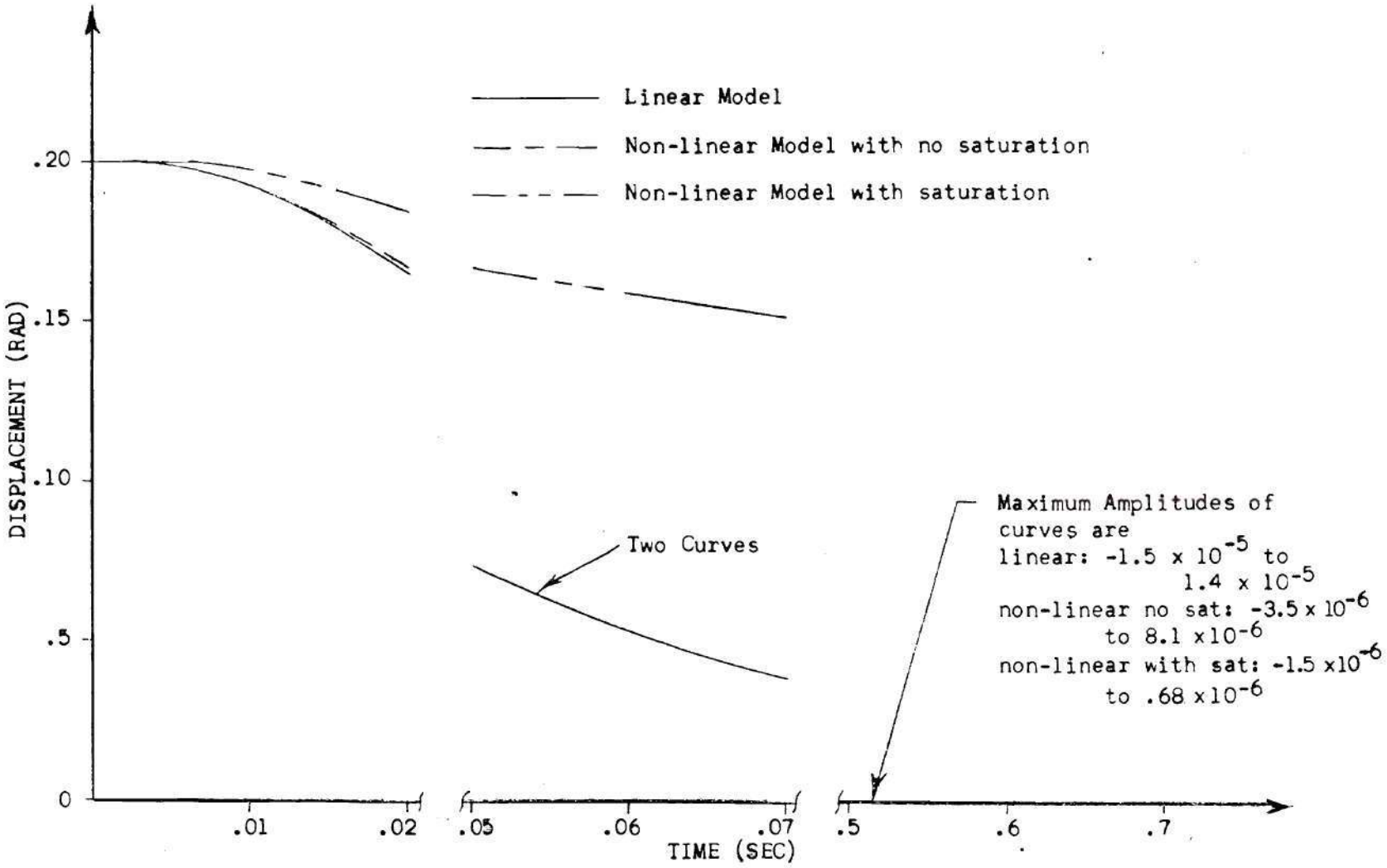


Figure 27. Turntable Displacement for Various Models.

making a recording of two system variables simultaneously. Unfortunately, local noise affected the instruments and subtle, rapid changes were impossible to detect. With a sine wave of varying frequency as an input, the response of the system was measured for both cylinder pressure and turntable displacement. When these recordings were compared with the theoretical response of the system, the correlation was very good. Graphs of actual and theoretical displacement are given in Figures 28 and 29. The input function to which the system in Figures 28 through 30 is subjected is a sine wave of a .0175 rad. amplitude which begins at the origin and ends at the time at which the data curves stop. The frequencies chosen for the comparison were considered representative points in the frequency range from .1 to 10 cycles per second (cps). Below .1 cps, attenuation and phase lag are negligible. Above 10 cps, the lack of resolution of the recording device made any measurement impossible. A calibration table was not available for the pressure transducer and it is only possible in Figure 30 to compare the shapes of the actual and theoretical pressure curves. The similarity of the curves serves as a further indication that the model is indeed correct. Being production items of Scientific-Atlanta, shipping schedules necessarily limited the testing availability of the positioners.

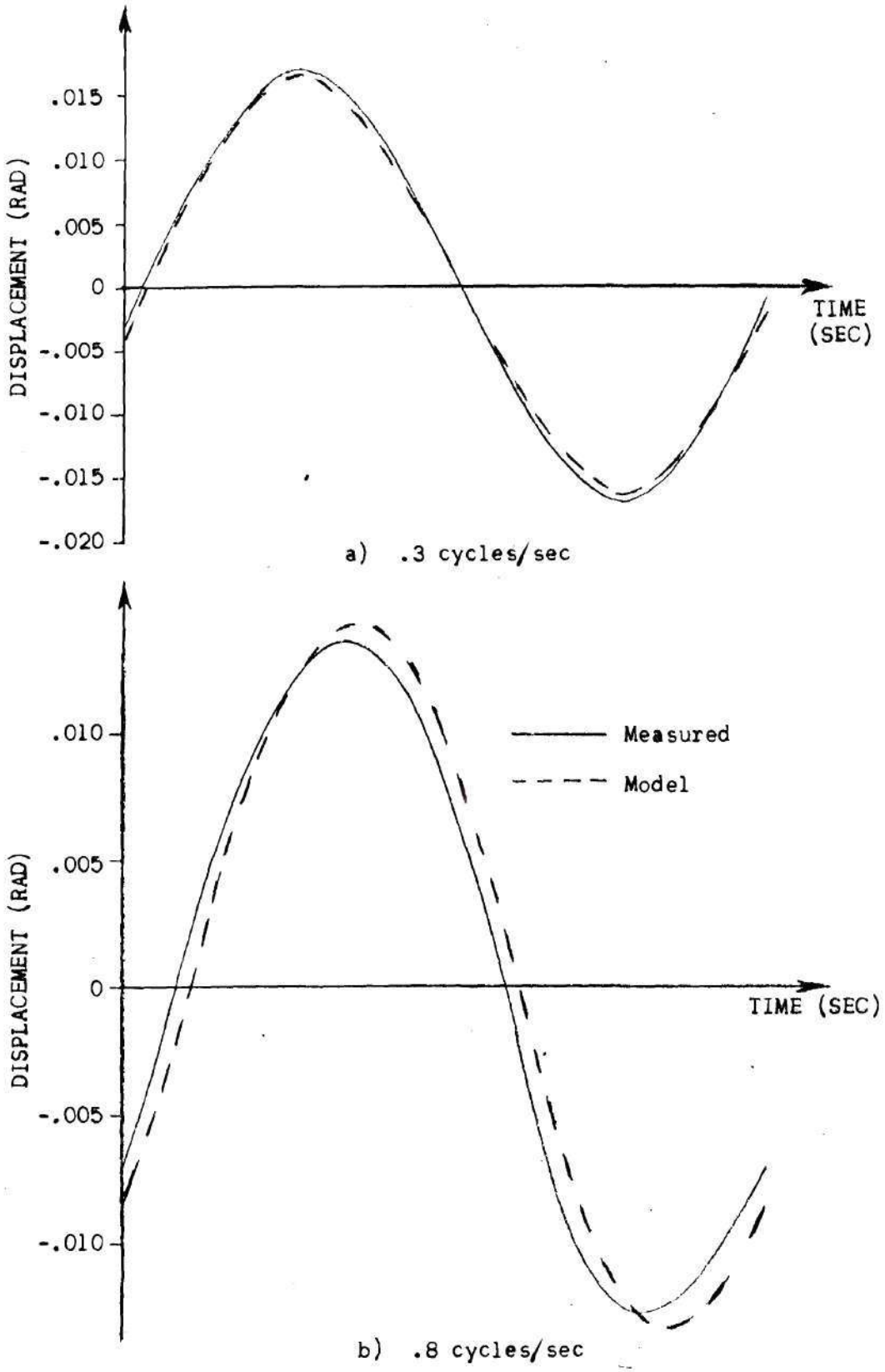


Figure 28. Comparison of Actual and Predicted Angular Displacements for Two Input Frequencies.

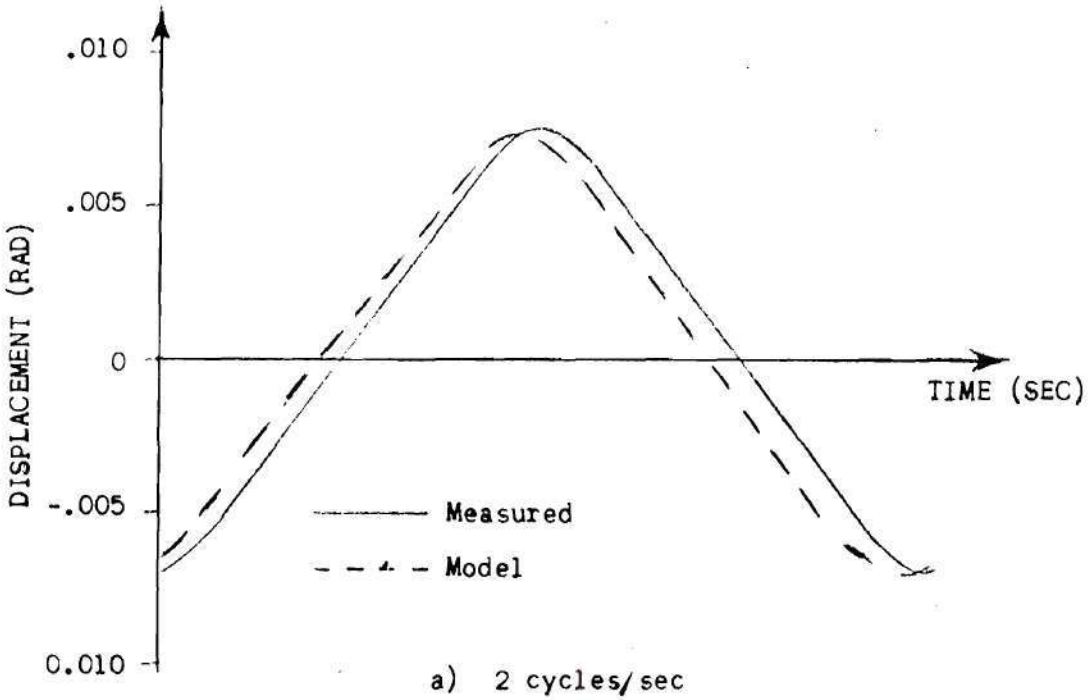


a) 2 cycles/sec

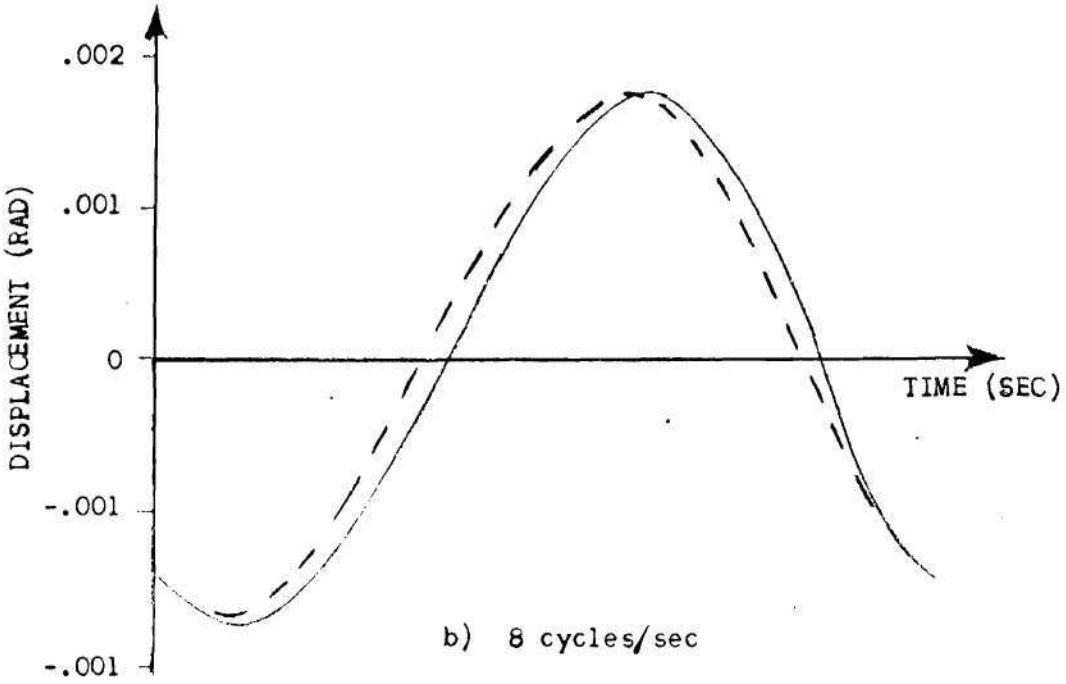


b) 8 cycles/sec

Figure 29. Comparison of Actual and Predicted Angular Displacements for Two Input Frequencies.

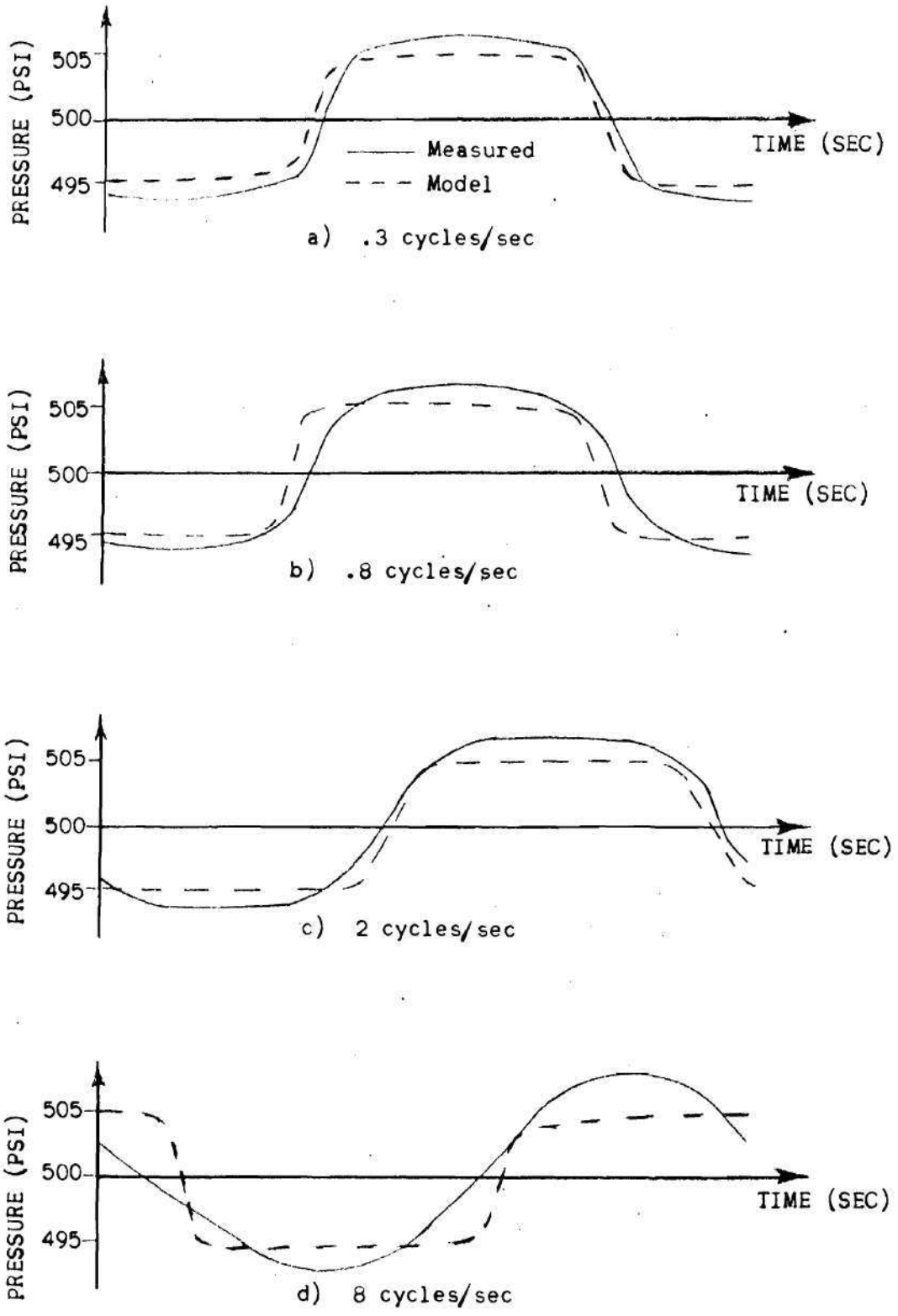


Figure 30. Comparison of Actual and Predicted Cylinder Pressure for Four Input Frequencies.

# CHAPTER IV

## CONCLUSIONS AND RECOMMENDATIONS

As a result of this study, a number of conclusions may be drawn regarding the modeling and performance of this hydraulic system.

Based upon the limited test data available, the non-linear model as presented above seems to be a good representation of the actual system.

A linear model of the system will not be accurate except for very small deviations between the desired and actual displacement.

The major performance limitation of the system is the relatively small maximum angular velocity of the turntable. Flow saturation of the valves and/or current saturation of the controller are the factors contributing to this condition.

The non-linear representation of the system has a very desirable apparent damping which reduces pressure oscillations for a large step input. This effect is due to the non-linear orifice flow relation of the spool valve and may be crudely approximated in the linear model by a leakage between the pistons.

Variations, within a range that might reasonably be expected to occur, in load inertia, viscous bearing friction, and leakage of the cylinder can have a significant effect on the cylinder pressure, but their effect is not significant with regard to turntable motion.

A few recommendations are made regarding further analytical work

on this problem and regarding future positioners to be built.

Hydraulic valves with a larger flow capacity, matched with the appropriate controller, could greatly improve the speed of response of the actual system. The substitution of these larger flow capacity components should be considered seriously in the design of further such positioners.

In any work which may follow this, the following topics which may affect the system performance are recommended for investigation:

1. Line dynamics, the next most significant effect as determined in this study.
2. Nonlinearity and resolution errors of the feedback potentiometer transducer.
3. Nonlinearity and backlash of the gearing mechanism between the turntable and transducer.

# APPENDIX A

## COMPLETE VALVE MODEL

Two relatively complete representations of the particular valve considered here are the Merritt (14) and Moog (15) models. Though essentially the same, a few important considerations are unique to each model. Therefore, these two models have been combined into one more complete model.

The Merritt model can be represented by the block diagram of Figure 31a. The main drawback of the Merritt model is that it considers differential voltage as an input, rather than current. The relationship between input current and input voltage of the Merritt model is

$$\Delta i = \frac{2\mu_{eq}}{(R_c + r_p)(1 + \frac{S}{\omega_a})} - \frac{2k_b S\,\theta}{(R_c + r_p)(1 + \frac{S}{\omega_a})} \qquad (A.1)$$

Note: All variables defined in Figure 31a.

Input torque to the flapper of the valve is linearly related to input current by the constant $k_t$. The flow diagram can thus be simplified to Figure 31b. Because the pressure feedback loop is normally of little effect, this factor may be eliminated from the model. The constants $k_t$, $k_{qp}$, $k_f(r+b)$, and $A_v$ of the Merritt model are equivalent to $k_1$, $k_2$, $k_\omega$, and $A_s$ of the Moog representation, Figure 32a. Incorporating the above changes in Figure 31b will result in Figure 31c.

Since the transfer function desired is $\frac{X(S)}{i(S)}$ rather than $\frac{Q(S)}{i(S)}$,

the final term of the Moog model may be eliminated. This change is included in Figure 32b.

At this point, two discrepancies between the Merritt and Moog models become apparent. One is due to the lack of damping in the armature-flapper stage of the Merritt model and the other lies in the absence of spool dynamics in the Moog model.

The damping of the Merritt model is accomplished by the back EMF of the coils of the armature. This term is eliminated when input current is utilized rather than input voltage. Recall that the servoamplifier is designed to output current rather than voltage. Since the armature of the Merritt model is not suspended in hydraulic fluid, there can be no viscous damping. The armature of the actual valve, however, is indeed suspended in fluid. Since this is the case, the Moog armature-flapper dynamics were assumed a more valid representation of the valve.

In the Moog analysis, the differential pressure across the spool is assumed to be negligible during dynamic conditions. Because the validity of this questionable assumption was never established, the more complete second stage analysis of Merritt was utilized.

The final transfer function is a combination of the features judged more representative of the valve used. The block diagram is given in Figure 33. This fifth order model is represented by the transfer function

$$\frac{X_o(S)}{i(S)} = \frac{\frac{k_1 k_2}{K_f A_s}}{s\left(1 + \frac{2\zeta}{\omega_n} s + \left(\frac{s}{\omega_n}\right)^2\right)\left(1 + \frac{2\zeta_{hp}}{\omega_{hp}} s + \left(\frac{s}{\omega_{hp}}\right)^2\right) + \frac{k_\omega k_2}{k_f A_s}} \quad . \qquad (A.2)$$

A frequency response analysis of the valve using the above transfer function was made and is pictured in Figure 4. All of the data used to develop the plot was supplied by the manufacturer (16)(17).

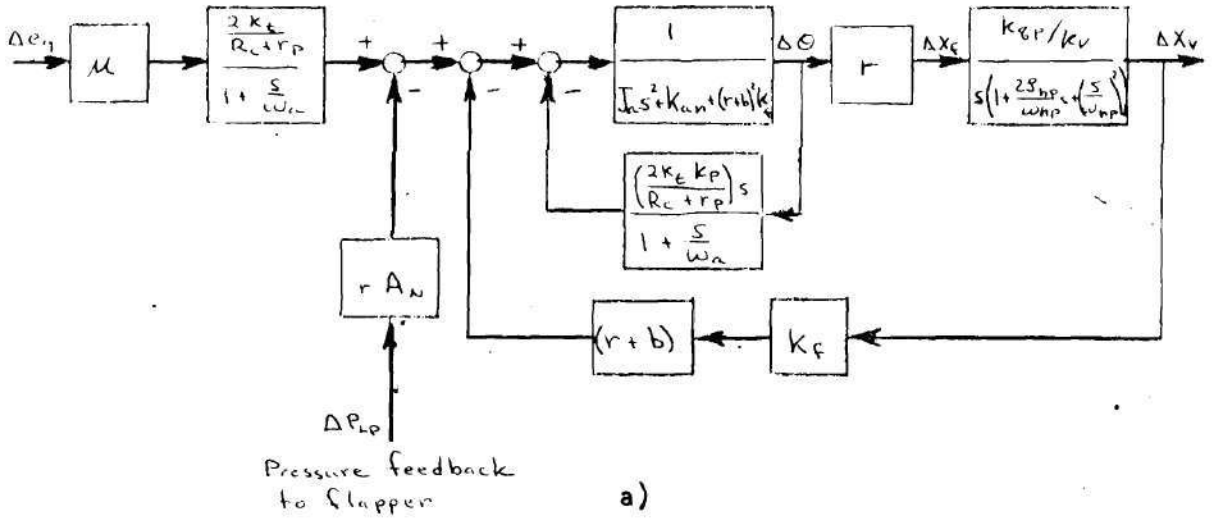


a)

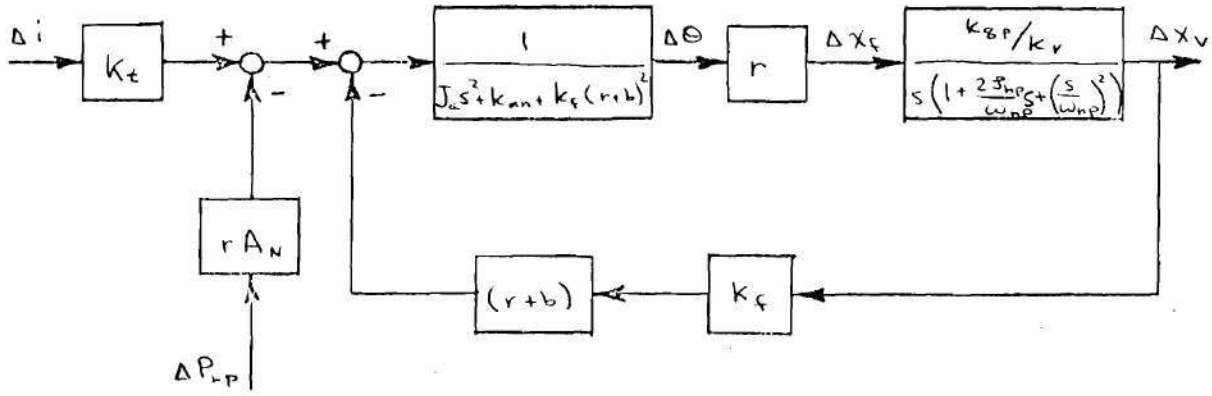


b)

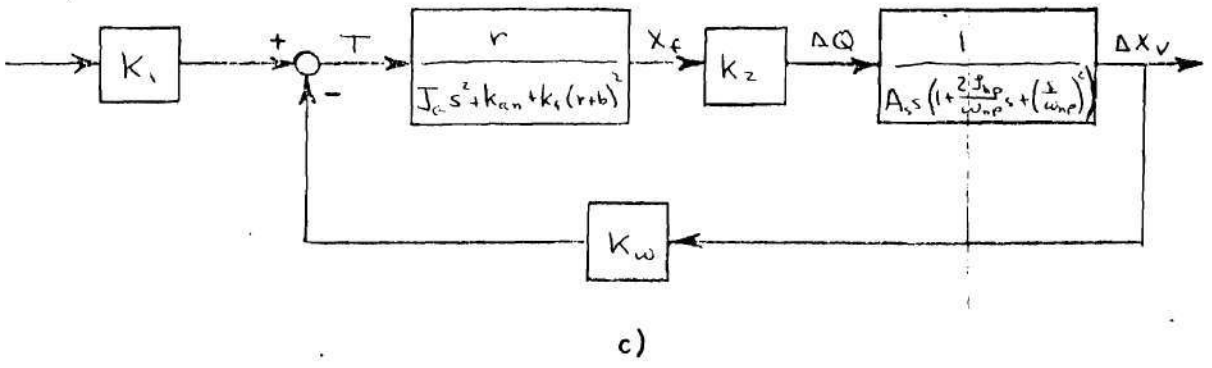


c)

**Figure 31. Flow Diagrams of Merrit Valve Model.**

where

$A_v$ = area of end of spool, $in^2$

$A_n$ = nozzle area, $in^2$

$b$ = distance between flapper nozzle and spool, in.

$k_{an}$ = net spring rate in-lb/rad

$k_f$ = spring constant of feedback spring, lb/in.

$k_{qp}$ = flow gain of flapper valve, $in^3$/sec/in

$k_t$ = torque constant of the torque motor, in-lb/amp

$J_a$ = inertia of the armature and any attached load, in lb $sec^2$

$r$ = distance between flapper pivot and flapper nozzle, in

$R_c$ = resistance in each coil, ohms

$r_p$ = internal (plate) resistance of amplifier in each coil circuit, ohms

$\omega_a$ = armature circuit break frequency

$\omega_{hp}$ = hydraulic natural frequency of pilot stage, rad/sec

$\zeta_{hp}$ = damping ratio of pilot stage, dimensionless

$\mu$ = amplifier gain for each side, dimensionless

$\Delta_{eg}$ = signal voltages from the amplifier, volts.

$\Delta\theta$ = angular displacement of flapper from null

$\Delta x_f$ = flapper displacement from null at nozzle

$\Delta x_v$ = spool displacement from null

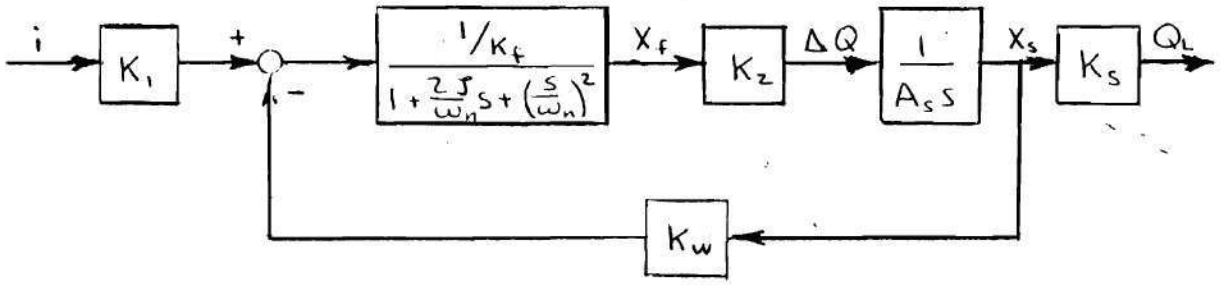


a)

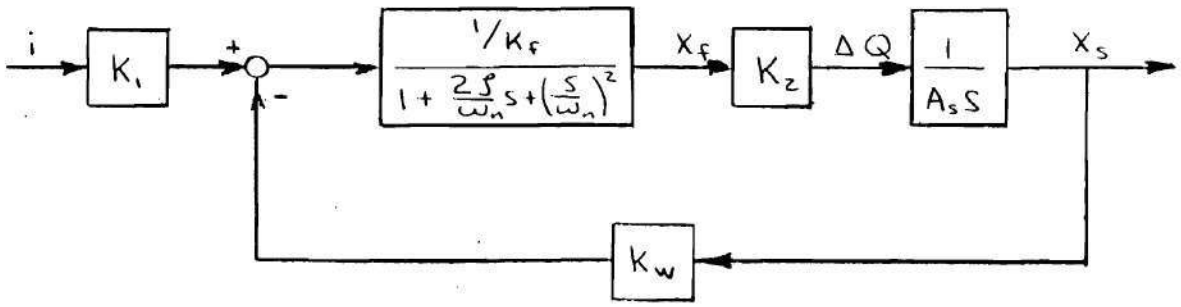


b)

Figure 32. Flow Diagrams of Moog Valve Model.

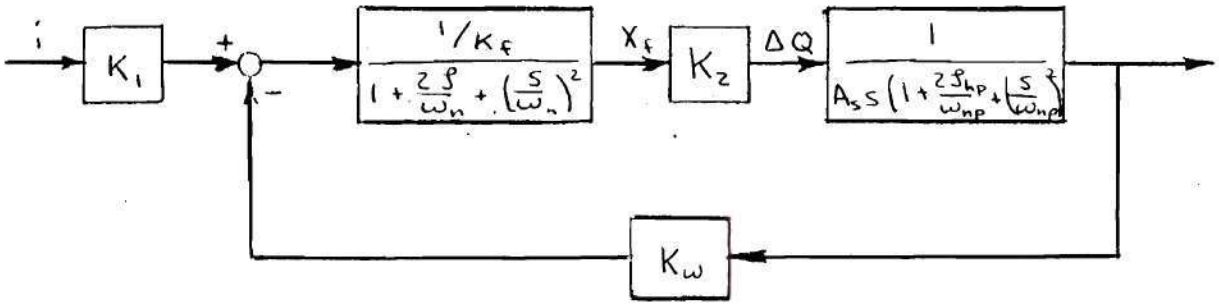


Figure 33. Flow Diagram of Composite Valve Model.

where

$A_s$ = spool end area, $in^2$.

$k_1$ = torque motor gain, in-lbf/ma.

$k_2$ = hydraulic amplifier flow gain, $in^3/sec/in$.

$k_3$ = flow gain of spool and bushing, $in^3/sec/in$

$k_f$ = net stiffness of armature - flapper, in-lbs/in.

$k_\omega$ = feedback wire stiffness, in-lbs/in.

$i$ = torque motor current, ma.

$\Delta Q$ = hydraulic amplifier differential flow, $in^3/sec$.

$Q_n$ = servovalve control flow, gpm.

$X_f$ = flapper displacement at nozzles, in.

$X_s$ = spool displacement, in.

$\zeta$ = damping ratio of first stage, dimensionless

$\omega_n$ = natural frequency of first stage, hz.

# APPENDIX B

## NONLINEAR COMPUTER PROGRAMS

Several subroutines were written to implement the nonlinear characteristics of the model. Each of these were called by function DYS, see Appendix D. All of the subroutines will be presented in the following paragraphs. Some require only a few words of explanation while others will be accompanied by a rather rigorous justification for the particular algarithms used. All programs were written in FORTRAN.

Subroutine SAT, Figure 34, is used to simulate saturation of the input IN. If the value of IN exceeds either MIN or MAX, OUT is set to the appropriate maximum and minimum. If IN lies between MIN and MAX, OUT will be IN.

Because voltage as well as current saturation were present in the controller, a numerical differentiation is used to determine the derivative of the current and hence the amplifier voltage. The technique used for the differentiation is a four-step Adams - Brashworth integration or a backward Newton integration (18). The backward integration was necessary because values for the current are known only for the past at any given time. Before the full four-step integration can take place, three previous values for current must be known. Lower order approximations are therefore used for these first three steps. These three values established, the four-step method is used. Error due to this method can be expressed as E, where

$$E = h^5\, y(\zeta)\left(\frac{251}{720}\right)$$

h = step size

$y(\zeta)$ = the fifth derivative of the current function at some point $\zeta$

Error by this method is extremely small.

The complete expression for voltage is

$$V = L\, di/dt + Ri$$

where V = voltage, volt.

L = coil inductance, henrys.

R = coil resistance, ohms.

i = current, amp.

If the voltage thus determined does not exceed the voltage limits, the current as determined by the numerical integration is accepted as the current output. If the voltage limit is exceeded, the saturation voltage must be integrated to determine the actual current. This may be accomplished as follows:

$$i = \frac{v_{sat}}{(LS + R)}$$

$$v_{sat} = i(LS + R)$$

$$\frac{Vsat}{L} - \frac{Ri}{L} = Si$$

$$i = (i)(step) + lasti$$

where S = laplacian operator

step = integration step size

lasti = last value of current

$$i = lasti + (\frac{v_{sat}}{L})(step) - (\frac{R}{L})(step)$$

$$i(1 + (\frac{R}{L})(step)) = lasti + \frac{v_{sat}}{L}(step)$$

$$i = \frac{(Lasti + (\frac{v_{sat}}{L})(step))}{(1 + (\frac{R}{L})(step))}$$

The above equation is then implemented to find the actual output current for voltage saturation. Figure 35 is a listing of the program, VSAT implementing this procedure.

Subroutine FLOW, Figure 36, uses the square-root orifice laws of equation (2.4) to determine the flows to and from the valve. The spool displacement is determined by the saturation scheme of Figure 5. This is implemented in the first segment of function DY.

The denominator of equation (2.13) is created in subroutine DENOM, Figure 37, and used in the program PDOT, Figure 38 to create the time derivative of pressure in equation (2.13).

The final nonlinearity is a characteristic of the bearing friction. This function may be pictorially described by Figure 11. A mathematical representation of this function is a decaying exponential which is a maximum at the $\dot{\theta} = 0$ point and decays to the kinetic friction value as $\dot{\theta}$ increases. Subroutine BRING, Figure 39, uses the maximum and minimum frictional values and a term representing rate of decay to simulate this value. Negative values of $\dot{\theta}$ make the sign of the friction negative.

```
EIG-STAN*NONLIN.SAT
      1            SUBROUTINE SAT(MIN,MAX,IN,OUT)
      2            REAL MIN,MAX,IN
      3            IF(IN.GT.MAX) OUT = MAX
      4            IF(IN.LT.MIN) OUT = MIN
      5            IF(IN.LE.MAX.AND.IN.GE.MIN) OUT = IN
      6            RETURN
      7            END
```

Figure 34. Subroutine SAT.

```
EIG-STAN*NONLIN.VSAT
      1            SUBROUTINE VSAT(VMIN,VMAX,L,RIND,PAST,STEP,NI,IN,OUT)
      2            DIMENSION PAST(3)
      3            REAL L,IN
      4            IF(NI.LT.4) GO TO 2
      5            DERIV = ((11.*IN/6.)-(3.*PAST(1)+(3.*PAST(2)/2.)-PAST(3)/3.)/STEP
      6            GO TO 7
      7          2 IF(NI.LT.3) GO TO 3
      8            DERIV = ((3.*IN-4.*PAST(1)+PAST(2))/2.)/STEP
      9          7 PAST(3) = PAST(2)
     10            GO TO 4
     11          3 IF(NI.LT.2) GO TO 9
     12            DERIV = (IN-PAST(1))/STEP
     13          4 PAST(2) = PAST(1)
     14            GO TO 10
     15          9 DERIV = 0.
     16         10 IF((L*DERIV+RIND*IN).LE.VMAX) GO TO 5
     17            DERIV = VMAX/L
     18            OUT = (PAST(2) + DERIV*STEP)/(1.+(RIND*STEP)/L)
     19            GO TO 8
     20          5 IF((L*DERIV+RIND*IN).GE.VMIN) GO TO 6
     21            DERIV = VMIN/L
     22            OUT = (PAST(2) + DERIV*STEP)/(1.+(RIND*STEP)/L)
     23            GO TO 7
     24          6 OUT = IN
     25          8 NI = NI + 1
     26            PAST(1) = OUT
     27            RETURN
     28            END
```

Figure 35. Subroutine USAT.

```
EIG-STAN*NONLIN.FLOW
      1            SUBROUTINE FLOW(Y,ID,Q)
      2            DIMENSION Y(7)
      3            COMMON/DOTO/ACY,LCY,LCM,R,KA,BE,DS,DEADB,ISAT,SATV,L,XSSAT,PS,PR,
     4           1OMEGAN,KV,ZETA,INER,KB,KAM,LEAK,BMAX,BMIN,BGAIN,RIND
      5            REAL K1,K2,LCY,LCM,KA,ISAT,L,KV,INER,KB,KAM,LEAK
      6            XS = Y(2)
      7            S = 314.*DS
      8            P1 = Y(4)
      9            P2 = Y(5)
     10            IF(XS.LT.DEADB/2.) GO TO 10
     11            K1 = S
     12            K2 = 0.
     13            GO TO 30
     14         10 IF(XS.GT.-DEADB/2.) GO TO 20
     15            K1 = 0.
     16            K2 = S
     17            GO TO 30
     18         20 K1 = 0.
     19            K2 = 0.
     20         30 IF(PS.GE.P1) PSM1 = SQRT(PS-P1)
     21            IF(PS.LT.P1) PSM1 = -SQRT(P1-PS)
     22            IF(PS.GE.P2) PSM2 = SQRT(PS-P2)
     23            IF(PS.LT.P2) PSM2 = -SQRT(P2-PS)
     24            GO TO(1,2),ID
     25          1 P1MR = SQRT(P1-PR)
     26            Q = XS*(K1*PSM1+K2*P1MR)
     27            RETURN
     28          2 P2MR = SQRT(P2-PR)
     29            Q = -XS*(K2*PSM2+K1*P2MR)
     30            RETURN
     31            END
```

Figure 36. Subroutine Flow.

```
:EIG-STAN*NONLIN.DENOM
      1            SUBROUTINE DENOM(TH,THDOT,P,DENOM)
      2            COMMON/DOTD/ACY,LCY,LCH,R,KA,BE,DS,DEADB,ISAT,SATV,L,XSSAT,PS,PR,
      3           1OMEGAN,KV,ZETA,INER,KB,KAM,LEAK,BMAX,BMIN,BGAIN,RIND
      4            REAL LCY,LCH,KA,ISAT,L,KV,INER,KB,KAM,LEAK
      5            C = (ACY/KA)*(LCH-3.1415*R/2.+TH*TH)
      6            VOL = ACY*(LCY/2.+R*TH+P*C)
      7            DENOM = VOL/BE + C*ACY
      8            RETURN
      9            END
```

Figure 37. Subroutine DENOM

```
:EIG-STAN*NONLIN.PDOT
      1            SUBROUTINE PDOT(Q,THDOT,P,DENOM,PDOT)
      2            COMMON/DOTD/ACY,LCY,LCH,R,KA,BE,DS,DEADB,ISAT,SATV,L,XSSAT,PS,PR,
      3           1OMEGAN,KV,ZETA,INER,KB,KAM,LEAK,BMAX,BMIN,BGAIN,RIND
      4            REAL LCY,LCH,KA,ISAT,KV,L,INER,KB,KAM,LEAK
      5            PDOT = (Q-ACY*R*(1.+ACY*P/KA*THDOT-LEAK*P))/DENOM
      6            RETURN
      7            END
```

Figure 38. Subroutine PDOT

```
:EIG-STAN*NONLIN.BRING
      1            SUBROUTINE BRING(DOT,OUT)
      2            COMMON/DOTD/ACY,LCY,LCH,R,KA,BE,DS,DEADB,ISAT,SATV,L,XSSAT,PS,PR,
      3           1OMEGAN,KV,ZETA,INER,KB,KAM,LEAK,BMAX,BMIN,BGAIN,RIND
      4            REAL LCY,LCH,KA,ISAT,L,KV,INER,KB,KAM,LEAK
      5            OUT = BMIN+(BMAX-BMIN)*EXP(-BGAIN*ABS(DOT))
      6            OUT = OUT/(INER/(32.2*12.))
      7            IF(DOT.LE.0.) GO TO 10
      8            RETURN
      9         10 IF(DOT.GE.0.) GO TO 20
     10            OUT = -OUT
     11            RETURN
     12         20 OUT = 0.
     13            RETURN
     14            END
```

Figure 39. Subroutine BRING.

# APPENDIX C

## STATE VARIABLE FORMAT

In state variable format, all dynamic effects must be expressed in terms of first order derivatives. To accomplish this a set of n quantities called state variables are established, n being equal to the order of the system. The time derivatives of each of these state variables are expressed as functions of the state variables. In this form, a numerical integration may be readily performed on the system when an initial condition for each of the state variables is known.

A simple example of how these derivatives are formed may be seen in the following conversion of the transfer function G(s) into state variable format.

$$G(s) = \frac{\theta(s)}{I(s)} = \frac{k_1}{k_2 + k_3 s + s^2}$$

$$\ddot{\theta}(s) + k_3\dot{\theta}(s) + k_2(s) = k_1 I(s)$$

$$\ddot{\theta} = k_1 I(s) - k_3\dot{\theta}(s) - k_2\theta(s)$$

If $\dot{\theta}$ is called $\omega$

$$\dot{\theta} = \omega$$

$$\dot{\omega} = k_1 I(s) - k_3\omega(s) + k_2\theta(s)$$

These are the two state variable equations.

The state variable equations for the linear system of Figure 13 are given in Chapter II and III and are repeated here:

$$\dot{V}_s = k_{con}\omega_n^2 i - 2\zeta\omega_n V_s - \omega_n^2 x_s \qquad \text{(from Figure 5)}$$

$$\dot{x}_s = V_s \qquad \text{(from Figure 5)}$$

$$\dot{p}_A = \frac{q - (L + k5)p - k1\omega - k6\theta + k7}{k4} \qquad \text{(Eq. 3.1)}$$

where $k1 = AR(1 + \frac{p_o A}{k})$

$$k2 = (\frac{Lch - \pi R}{2} + \theta_o R)$$

$$k3 = q_o - Lp_o - k_1\omega_o$$

$$k4 = A^2/\beta \quad \frac{1}{k}(\beta + p_o)k_2 + 1/A(Lcy/2 + R\theta_o)$$

$$k5 = \frac{A^2/k(k4\ R\omega_o + \frac{k3k2}{\beta})}{k4}$$

$$k6 = \frac{A^2 kk3}{\beta k4} \quad (\frac{\beta + p_o}{k}) + \frac{1}{A}$$

$$k7 = k5p_o + k6\theta_o$$

$$\dot{p}_B = \frac{q - (L + k5)p - k1\omega - k6\theta + k7}{k4} \qquad \text{(Eq. 3.1)}$$

where q, $\theta$, and $\omega$ are of opposite sign for $\dot{p}_B$.

$$\dot{\omega} = \frac{AR(P_A - P_B) + M_{ext} - f(\omega) - k_B\omega}{I} \qquad (2.15)$$

$$\dot{\theta} = \omega \qquad (2.16)$$

In this case $v_s$, $x_s$, $p_A$, $p_B$, $\omega$, and $\theta$ are the state variables with the proper values for all of the constants included, the matrix state variable expression is

$$\begin{bmatrix} v_s \\ x_s \\ p_A \\ p_B \\ \omega \\ \theta \end{bmatrix} = \begin{bmatrix} 0 & 1 & 0 & 0 & 0 & 0 \\ -19600 & -252 & 0 & 0 & 0 & -513 \\ 6.E7 & 0 & -3.E-3 & 0 & -2.E+5 & 2.2 \\ -6.E7 & 0 & 0 & -3.E-3 & 2.E+5 & -2.2 \\ 0 & 0 & -11.5 & -11.5 & -1.E-2 & 0 \\ 0 & 0 & 0 & 0 & 0 & 0 \end{bmatrix} \begin{bmatrix} v_s \\ x_s \\ p_A \\ p_B \\ \omega \\ \theta \end{bmatrix} + \begin{bmatrix} 0 & 0 & 0 \\ 513 & 0 & 0 \\ 0 & 0 & 0 \\ 0 & 0 & -5.3E-4 \\ 0 & .154 & 0 \\ 0 & 0 & 0 \end{bmatrix} \begin{bmatrix} \theta_d \\ M_{ext} \\ 1 \end{bmatrix}$$

# APPENDIX D

## LINEAR AND NON-LINEAR COMPUTER PROGRAMS

Several computer programs were developed to digitally implement the linear and non-linear models as were presented in Chapter II.

The first four programs are the non-linear programs. The main program, INTEG, serve a an interface between the operator and the computer. Here, the integration step size, initial conditions, system inputs, and final time are input. The output includes information regarding the system states at predetermined time intervals. The program labelled CONSTANTS stores all of the system constants. Program AB assigns all of the linear elements of the A and B matrices. Subfunction DYS is used by the Runge-Kutta numerical integration to establish the time derivatives of each of the state variables. This function calls each of the non-linear subroutines described in Appendix B.

The linear model is made up of the second group of four programs The main program, INTEG, serves the same purpose as the main non-linear program. In addition, the linearization point is entered in this program. Data representing the system parameters is again stored in CONSTANTS. Subfunction DYS forms the time derivatives of the state variables using the A and B matrices created by the fourth linear subroutine LINA. LINA creates the A and B matrices which are described by the linearized system equations.

```
EIG-STAN•NONLIN,INTEG
      1            DIMENSION Y(7),Z(7),G(7),A(6,6),B(6,2),PAST(3)
      2            EXTERNAL DY
      3            COMMON/DOTS/A,B,AMPTHD,CPSTHD,AMPMEX,CPSMEX,PHAMEX,PAST,
      4           1STEP,NI
      5        100 FORMAT()
      6            ID = 0
      7         10 WRITE(6,101)
      8        101 FORMAT(' ENTER RKDE AND PRINT STEP SIZE AND FINAL TIME')
      9            READ(5,100)H,Z,ZF
     10            WRITE(6,100)H,Z,ZF
     11            WRITE(6,105)
     12        105 FORMAT(' ENTER AMPLITUDE AND FREQUENCY(CPS) OF THETA',
     13           1' DESIRED AND AMPLITUDE,',',' FREQUENCY(CPS), AND PHASE',
     14           2' SHIFT OF EXTERNAL MOMENT.')
     15            READ(5,100)AMPTHD,CPSTHD,AMPMEX,CPSMEX,PHADEG
     16            WRITE(6,100)AMPTHD,CPSTHD,AMPMEX,CPSMEX,PHADEG
     17            PHAMEX = PHADEG/57.27578
     18            WRITE(6,102)
     19        102 FORMAT(' ENTER INITIAL VECTOR WITH INITIAL TIME FIRST.')
     20            READ(5,100)Y
     21            WRITE(6,100)Y
     22            CALL AB(A,B,ID)
     23            THETA0 = Y(7)
     24            STEP = H/4.
     25            NI = 1
     26            EPSIL = H/10.
     27            Z0 = Y(1)
     28            WRITE(6,106)
     29        106 FORMAT(4X,'TIME',6X,'A-CYLINDER',3X,'B-CYLINDER',3X,'THETA DOT',
     30           1 7X,'THETA')
     31            WRITE(6,100)Y(1),Y(4),Y(5),Y(6),Y(7)
     32         20 Z0 = Z0 + Z
     33            CALL RKDE(DY,Y,Z0,H,W,0,7)
     34            IF(Y(4).LT.0.) Y(4) = 0.
     35            IF(Y(5).LT.0.) Y(5) = 0.
     36            WRITE(6,100)Y(1),Y(4),Y(5),Y(6),Y(7)
     37            IF(Z0.LT.ZF-EPSIL) GO TO 20
     38         30 WRITE(6,103)
     39        103 FORMAT(' DO YOU WISH TO CONTINUE(1), START OVER(2), OR STOP(3)')
     40            READ(5,100)ID
     41            IF(ID.EQ.2) GO TO 10
     42            IF(ID.EQ.3) GO TO 40
     43            WRITE(6,104)
     44        104 FORMAT(' ENTER RKDE AND PRINT STEP SIZE AND FINAL TIME')
     45            READ(5,100)HN,Z,ZF
     46            WRITE(6,100)HN,Z,ZF
     47            STEP = H/4.
     48            IF(ABS(HN-H).LT.10.E-6) GO TO 20
     49            H = HN
     50            NI = 1
     51            GO TO 20
     52         40 STOP
     53            END
```

```
EIG-STAN•NONLIN,CONSTANTS
      1            COMPILER(DATA=SHORT),(DATA=IBM)
      2            BLOCK DATA
      3            REAL LCY,LCH,KA,KV,L,INER,KB,KAM,ISAT,LEAK
      4            COMMON/DOTS/ACY,LCY,LCH,R,KA,BE,DS,DEADB,ISAT,SATV,L,XSSAT,PS,PR,
      5           1OMEGAN,KV,ZETA,INER,KB,KAM,LEAK,RMAX,RMIN,RGAIN,RIND
      6            DATA ACY,LCY,LCH,R,KA,BE,DS/5.16,13.75,53.95,14.33,2.E6,2.7E5,.312/
      7            DATA KB,DEADB,ISAT,SATV,L,XSSAT,PS/.1,0.,50.,10000.,1.,.0025,1000./
      8            DATA INER,OMEGAN,KV,ZETA,LEAK,PR/2500.,140.,.25666,.9,1.E-6,0./
      9            DATA KAM,RMAX,RMIN,RGAIN,RIND/2000.,780.,660.,10.,200./
     10            END
```

EIG-STAN*NONLIN.A3

```
      SUBROUTINE A3(A,B,II)
      DIMENSION A(6,6),B(6,2)
      COMMON/DOTD/ACY,LCY,LCH,R,KA,BE,DS,DEADB,ISAT,SATV,L,XSSAT,PS,PR,
     1OMEGAN,KV,ZETA,INER,KB,KAM,LEAK,BMAX,BMIN,HGAIN,RIND
      READ LCH,L,LCY,INER,KA,KV,KB,ISAT,KAM,LEAK
  100 FORMAT()
      WRITE(6,101)
  101 FORMAT(' DO YOU WISH A PRINTOUT OF A AND B? 1=YES, 2=NO')
      READ(5,100)ID
      DO 20 I=1,6
      DO 30 J=1,6
      A(I,J) = 0.
   30 CONTINUE
      DO 20 J=1,2
      B(I,J) = 0
   20 CONTINUE
      IF(II.NE.0) GO TO 15
      CONST = DS*314.*SQRT((PS-PR)/2.)
      KV = KV/CONST
      II = 1
   15 A(1,2) = 1.
      A(2,1) = -(OMEGAN**2.)
      A(2,2) = -2.*ZETA*OMEGAN
      A(2,6) = -KAM
      A(5,3) = ACY*R/(INER/(32.2*12.))
      A(5,4) = -ACY*R/(INER/(32.2*12.))
      A(5,5) = -KB/(INER/(32.2*12.))
      A(6,5) = 1.
      B(2,1) = KAM
      B(5,2) = 1/(INER/(32.2*12.))
      IF(ID.EQ.2) GO TO 60
      WRITE(6,103)
  103 FORMAT(' A MATRIX')
      DO 40 I=1,6
      WRITE(6,100)(A(I,J),J=1,6)
   40 CONTINUE
      WRITE(6,104)
  104 FORMAT(' B MATRIX')
      DO 50 I=1,6
      WRITE(6,100)(B(I,J),J=1,2)
   50 CONTINUE
   60 RETURN
      END
```

EIG-STAN*NONLIN.DYS

```
      FUNCTION DY(T,I)
      DIMENSION Y(7),A(6,6),B(6,2),PAST(3)
      COMMON/DOTS/A,B,AMPTHD,CPSTHD,AMPMEX,CPSMEX,PHAMEX,PAST,
     1STEP,NI
      COMMON/DOTD/ACY,LCY,LCH,R,KA,BE,DS,DEADB,ISAT,SATV,L,XSSAT,
     1PS,PR,OMEGAN,KV,ZETA,INER,KB,KAM,LEAK,BMAX,BMIN,HGAIN,RIND
      REAL LCY,LCH,KA,ISAT,L,IOPT,IMAX,ICORR,KV,INER,KB,KAM,LEAK
      GO TO (1,2,3,4,5,6),I
    1 IF(ABS(Y(2)).LE.XSSAT.OR.Y(3)*SIGN(1.,Y(2)).LE.0.) GO TO 10
      Y(2) = SIGN(XSSAT,Y(2))
      Y(3) = 0.
   10 DY = A(1,2)*Y(3)
      RETURN
    2 IOPT = A(2,6)*Y(7)+AMPTHD*SIN(6.2832*CPSTHD*Y(1))*B(2,1)
      CALL SAT(-ISAT,ISAT,IOPT,IMAX)
      CALL VSAT(-SATV,SATV,L,RIND,PAST,STEP,NI,IMAX,ICORR)
      DY = A(2,1)*Y(2)+A(2,2)*Y(3)+ICORR*KV*(OMEGAN**2.)
      RETURN
    3 IF(Y(4).LT.0.) Y(4) = 0.
      CALL FLOW(Y,1,Q)
C     REMOVE 'C' OF NEXT LINE TO REMOVE SQUARE LAW ORIFICES
C     Q = Y(2)*314*DS*SQRT((PS-PR)/2.)
      CALL DENOM(Y(7),Y(6),Y(4),DEN)
      CALL PDOT(Q,Y(6),Y(4),DEN,DOT)
      DY = DOT
      RETURN
    4 IF(Y(5).LT.0.) Y(5) = 0.
      CALL FLOW(Y,2,Q)
C     REMOVE 'C' OF NEXT LINE TO REMOVE SQUARE LAW ORIFICES
C     Q = -Y(2)*314*DS*SQRT((PS-PR)/2.)
      CALL DENOM(-Y(7),-Y(6),Y(5),DEN)
      CALL PDOT(Q,-Y(6),Y(5),DEN,DOT)
      DY = DOT
      RETURN
    5 CALL URINSTY(6,OUT)
C     REMOVE 'C' OF NEXT LINE TO ELIMINATE NONLINEAR BEARING FRICTION
C     OUT = 0.
      DY = A(5,3)*Y(4)+A(5,4)*Y(5)+A(5,5)*Y(6)+B(5,2)*AMPMEX*
     1SIN(6.2832*CPSMEX*Y(1)+PHAMEX)-OUT
      RETURN
    6 DY = A(6,5)*Y(6)
      RETURN
      END
```

```
ZEIG-STAN-LIN.INITS
      1             DIMENSION Y(7),Y0(7),W(7),Q(7),A(6,6),B(6,3)
      2             EXTERNAL DY
      3             COMMON/DUTS/A,B,AMPTHD,CPSTHD,AMPMEX,CPSMEX,PHAMEX
      4         100 FORMAT()
      5          10 WRITE(6,101)
      6         101 FORMAT(' ENTER RKDE AND PRINT STEP SIZE AND FINAL TIME.')
      7             READ(5,100)H,Z,ZF
      8             WRITE(6,100)H,Z,ZF
      9             WRITE(6,105)
     10         105 FORMAT(' ENTER AMPLITUDE AND FREQUENCY(CPS) OF THETA'
     11            1' DESIRED AND AMPLITUDE','/,' FREQUENCY(CPS), AND PHASE'
     12            2' SHIFT OF EXTERNAL MOMENT.')
     13             READ(5,100)AMPTHD,CPSTHD,AMPMEX,CPSMEX,PHADEG
     14             WRITE(6,100)AMPTHD,CPSTHD,AMPMEX,CPSMEX,PHADEG
     15             PHAMEX = PHADEG/57.27578
     16             WRITE(6,104)
     17         104 FORMAT(' ENTER LINEARIZATION POINT')
     18             READ(5,100)X
     19             WRITE(6,100)X
     20             WRITE(6,102)
     21         102 FORMAT(' ENTER INITIAL VECTOR WITH INITIAL TIME FIRST.')
     22             READ(5,100)Y
     23             WRITE(6,100)Y
     24             THETA0 = Y(7)
     25             CALL LINA(X,A,B)
     26             EPSIL = H/10.
     27             Z0 = Y(1)
     28             WRITE(6,100)Y(1),Y(2),Y(4),Y(5),Y(6),Y(7)
     29          20 Z0 = Z0 + Z
     30             CALL RKDE(DY,Y,Z0,H,W,Q,7)
     31             WRITE(6,100)Y(1),Y(2),Y(4),Y(5),Y(6),Y(7)
     32             IF(Z0.LT.ZF-EPSIL) GO TO 20
     33          30 WRITE(6,103)
     34         103 FORMAT(' DO YOU WISH TO CONTINUE(1), START OVER(2), OR STOP(3)')
     35             READ(5,100)ID
     36             IF(ID.EQ.2) GO TO 10
     37             IF(ID.EQ.3) GO TO 40
     38             WRITE(6,106)
     39         106 FORMAT(' ENTER RKDE AND PRINT STEP SIZE AND FINAL TIME.')
     40             READ(5,100)H,Z,ZF
     41             WRITE(6,100)H,Z,ZF
     42             GO TO 20
     43          40 STOP
     44             END
```

```
ZEIG-STAN-LIN.CONSTANTS
      1             BLOCK DATA
      2             COMMON/CONST/ACY,KA,R,LCH,LCY,BE,OMEGAN,ZETA,KV,INER,KB,KAM
      3             REAL LCH,LCY,INER,KA,KV,KB,L,KAM
      4             DATA ACY,KA,LCH,LCY,BE/5.16,2.E+6,57.05,27.5,2.7E+5/
      5             DATA OMEGAN,ZETA,KV,R/140.,.9,.2566A,14.33/
      6             DATA KAM,L,KB,INER/2000.,1.E-6,.1,2500./
      7             END
```

```
ZEIG-STAN-LIN.DYS
      1             FUNCTION DY(Y,I)
      2             COMMON/DUTS/A,B,AMPTHD,CPSTHD,AMPMEX,CPSMEX,PHAMEX
      3             DIMENSION Y(7),A(6,6),B(6,3)
      4             DY = 0.
      5             DY = A(I,1)*Y(2)+A(I,2)*Y(3)+A(I,3)*Y(4)+A(I,4)*Y(5)+A(I,5)*Y(6)
      6             DY = DY + A(I,6)*Y(7)+B(I,1)*AMPTHD*SIN(6.2832*CPSTHD*Y(1))
      7             DY = DY + B(I,2)*AMPMEX*SIN(6.2832*CPSMEX*Y(1)+PHAMEX) + B(I,3)
      8             RETURN
      9             END
```

```
ZEIG-STAN-LIN.LINA
      1            SUBROUTINE LINAT(X,A,B)
      2            DIMENSION KF(7),KR(7),A(6,6),B(6,3),X(6)
      3            COMMON/CONST/ACY,KA,R,LCH,LCY,BE,OMEGAN,ZETA,KV,INER,KB,KAM
      4            REAL LCH,LCY,INER,KB,KV,KA,KF,KR,KAM
      5            DEFINE K1(P0) = (1+ACY*P0/KA)*ACY*R
      6            DEFINE K2(TH0) = ((LCH-3.1416*R)/2.)+TH0*R
      7            DEFINE K3(Q0,P0,THDOT0,K1) = Q0-L*P0-K1*THDOT0
      8            DEFINE K4(TH0,P0,K2) = (ACY**2./BE)*((LCY/2.+R*TH0)/ACY+K2*(P0+BE
     9           1/KA)
     10            DEFINE K5(THDOT0,K2,K3,K4)=(K4*R*THDOT0+K2*K3/BE)*(ACY**2./(KA*K4
     11           1)
     12            DEFINE K6(K3,K4,P0) = ((R*ACY**2./BE)*(1/ACY+(P0+BE)/KA)+K3/K4)
     13            DEFINE K7(K5,K6,P0,TH0) = K5*P0+K6*TH0
     14       100 FORMAT()
     15            WRITE(6,101)
     16       101 FORMAT(' DO YOU WISH A PRINTOUT OF A AND B? 1=YES, 0=NO')
     17            READ(5,100)ID
     18            PF0 = X(3)
     19            PR0 = X(4)
     20            QF0 = X(1)*(OMEGAN**2.)*KV
     21            QR0 = -X(1)*(OMEGAN**2.)*KV
     22            TH0 = X(6)
     23            THDOT0 = X(5)
     24            KF(1) = K1(PF0)
     25            KF(2) = K2(TH0)
     26            KF(3) = K3(QF0,PF0,THDOT0,KF(1))
     27            KF(4) = K4(TH0,PF0,KF(2))
     28            KF(5) = K5(THDOT0,KF(2),KF(3),KF(4))
     29            KF(6) = K6(KF(3),KF(4),PF0)
     30            KF(7) = K7(KF(5),KF(6),PF0,TH0)
     31            KR(1) = K1(PR0)
     32            KR(2) = K2(-TH0)
     33            KR(3) = K3(QR0,PR0,-THDOT0,KR(1))
     34            KR(4) = K4(-TH0,PR0,KR(2))
     35            KR(5) = K5(-THDOT0,KR(2),KR(3),KR(4))
     36            KR(6) = K6(KR(3),KR(4),PR0)
     37            KR(7) = K7(KR(5),KR(6),PR0,-TH0)
     38            IF(ID.EQ.2) GO TO 10
     39            WRITE(6,100)(KF(I),I=1,7)
     40            WRITE(6,100)(KR(I),I=1,7)
     41         10 DO 20 I=1,6
     42            DO 30 J=1,6
     43            A(I,J) = 0.
     44         30 CONTINUE
     45            DO 20 J=1,3
     46            B(I,J) = 0
     47         20 CONTINUE
     48            A(1,2) = 1.
     49            A(2,1) = -(OMEGAN**2.)
     50            A(2,2) = -2.*ZETA*OMEGAN
     51            A(2,6) = -KAM*KV
     52            A(3,1) = (OMEGAN**2.)/KF(4)
     53            A(3,3) = -(1+KF(5))/KF(4)
     54            A(3,5) = -KF(1)/KF(4)
     55            A(3,6) = -KF(6)/KF(4)
     56            A(4,1) = -(OMEGAN**2.)/KR(4)
     57            A(4,4) = -(1+KR(5))/KR(4)
     58            A(4,5) = +KR(1)/KR(4)
     59            A(4,6) = +KR(6)/KR(4)
     60            A(5,3) = ACY*R/(INER/(32.2*12.))
     61            A(5,4) = -ACY*R/(INER/(32.2*12.))
     62            A(5,5) = -KB/(INER/(32.2*12.))
     63            A(6,5) = 1.
     64            B(2,1) = KAM*KV
     65            B(3,3) = KF(7)/KF(4)
     66            B(4,3) = KR(7)/KR(4)
     67            B(5,2) = 1/(INER/(32.2*12.))
     68            IF(ID.EQ.2) GO TO 60
     69            WRITE(6,103)
     70       103 FORMAT(' A MATRIX')
     71            DO 40 I=1,6
     72            WRITE(6,100)(A(I,J),J=1,6)
     73         40 CONTINUE
     74            WRITE(6,104)
     75       104 FORMAT(' B MATRIX')
     76            DO 50 I=1,6
     77            WRITE(6,100)(B(I,J),J=1,3)
     78         50 CONTINUE
     79         60 RETURN
     80            END
```

## REFERENCES


1. Blackburn, J. F. et al., Fluid Power Control, The Technology Press of M.I.T. and John Wiley and Sons, Inc., New York, 1960.

2. Ransch, R. G., "The Analysis of Valve Controlled Hydraulic Servomechanisms," The Bell System Technical Journal, November, 1959.

3. Merritt, H. E., Hydraulic Control Systems, John Wiley and Sons, Inc., New York, 1967, p. 215.

4. Thayer, W. J., "Technical Bulletin 103," Moog Servocontrollers Inc., East Aurora, New York, January, 1965, p. 8.

5. Thayer, Ibid, p. 4.

6. Blackburn, Ibid, p. 186.

7. Merritt, Ibid, p. 42

8. Merritt, Ibid, p. 6.

9. Merritt, Ibid, p. 68.

10. Blackburn, Ibid, p. 138.

11. Blackburn, Ibid, p. 134.

12. Takahashi, Yasundo, et al., Control and Dynamic Systems, Addison-Wesley Publishing Co., Reading, Mass., 1970, p. 44.

13. Conte, S. D. and de Boor, Carl, Elementary Numerical Analysis, McGraw Hill, New York, 1972, p. 382.

14. Merritt, Ibid, p. 215.

15. Thayer, Ibid, p. 8.

16. Thayer, Ibid, p. 9.

17. Maskrey, Robert H., Section Head, Moog Servocontrols Inc., Personal Conversation, Aug. 19, 1973.

18. Conte, Ibid, p. 341.